



Christoph Mayer, BSc

Application of Discrete Markov Chains to Thermodynamic Modeling of Lattice Systems

MASTER'S THESIS

to achieve the university degree of

Diplom-Ingenieur

Master's degree programme: Chemical and Process Engineering

submitted to

Graz University of Technology

Supervisor

Ass.Prof. Dipl.-Ing. Dr.techn. Thomas Wallek

Institute of Chemical Engineering and Environmental Technology

AFFIDAVIT

I declare that I have authored this thesis independently, that I have not used other than the declared sources/resources, and that I have explicitly indicated all material which has been quoted either literally or by content from the sources used. The text document uploaded to TUGRAZonline is identical to the present master's thesis.

Date

Signature

Acknowledgement

I would like to thank Prof. R. Tichy and Prof. A. Pfennig for inspiring discussions.

I owe my deepest gratitude to my supervisor Prof. T. Wallek for always taking the time to answer my questions immediately, providing guidance, and for always being optimistic about finding a promising result.

Kurzfassung

Thermodynamische Eigenschaften von kondensierten Fluiden im Gleichgewicht werden durch diskrete Zustände von Molekülen im Gittersystem und deren direkte Nachbarn gemeinsam mit der Shannon-Entropie beschrieben. Diese Arbeit beschäftigt sich mit der Weiterentwicklung eines von Vinograd entwickelten Modells, welches auf einem sequenziellen Gitteraufbau beschrieben mit Hilfe von Markov Ketten basiert. Die existierende zweidimensionale Methode wird auf drei Dimensionen erweitert und auf das kubisch primitive Gitter angewendet. Weiters ist auch die Genauigkeit bezüglich Monte Carlo Simulationen verbessert. Das resultierende Modell stellt einen Fortschritt gegenüber der häufig verwendeten quasichemischen Approximation von Guggenheim dar und entspricht damit einer aussichtsreichen Basis für ein zukünftiges g^E Modell.

Abstract

Thermodynamic properties of condensed-phase lattice fluids in equilibrium are described using discrete states of molecules and their respective neighbors in conjunction with Shannon entropy. This work is focused on further developing a model proposed by Vinograd, which is based on the description of a sequential lattice construction using discrete Markov chains. The existing two-dimensional method is extended to three dimensions and applied to the simple cubic lattice. Furthermore, the accuracy compared to Monte Carlo simulations is improved. The resulting model presents an improvement over the frequently used quasi-chemical theory proposed by Guggenheim and therefore provides a promising basis for future g^E -model development.

Contents

1. Introduction	1
2. General	3
2.1. Stochastic Basics and Nomenclature	3
2.2. Thermodynamic Basics	4
2.2.1. Quasi-chemical Approximation	5
2.3. Thermodynamic Consistency	6
2.4. Monte Carlo Simulations	7
2.5. Model Development using Wolfram Mathematica	8
2.5.1. Applications and Packages	8
2.5.2. Manipulation of Systems of Equations	9
3. Chain Lattice (1D)	10
3.1. Minimization of the Helmholtz free energy	12
3.2. Comparison to Guggenheim	14
4. Square Lattice (2D)	15
4.1. Vinograd's First Approximation	18
4.1.1. Comparison to Guggenheim and Monte Carlo Simulations	20
4.1.2. Thermodynamic Consistency Check	22
4.1.3. Asymmetry	23
4.2. Vinograd's Second Approximation	26
4.2.1. Comparison to Guggenheim and Monte Carlo Simulations	29
4.2.2. Thermodynamic Consistency Check	30
4.3. Refinement of Vinograd's Second Approximation	32
4.3.1. Comparison to Guggenheim and Monte Carlo Simulations	33
4.3.2. Thermodynamic Consistency Check	34
4.4. Comparison of Models	36
5. Simple Cubic Lattice (3D)	37
5.1. Vinograd's First Approximation Applied to 3D	39
5.1.1. Comparison to Guggenheim and Monte Carlo Simulations	40
5.1.2. Thermodynamic Consistency Check	41
5.2. Vinograd's Second Approximation Applied to 3D	43
5.2.1. Comparison to Guggenheim and Monte Carlo Simulations	48
5.2.2. Thermodynamic Consistency Check	49
5.3. Refinement of Vinograd's Second Approximation	51
5.3.1. Comparison to Guggenheim and Monte Carlo Simulations	53
5.3.2. Thermodynamic Consistency Check	54
5.4. Comparison of Models	56
6. Conclusion and Outlook	57
A. List of Symbols	58
List of Figures	59

Contents	vi
List of Tables	61
References	62

1. Introduction

Lattice models have long been an important tool for the description of condensed phases in the field of statistical mechanics. Some of their most common applications include the description of crystals and excess Gibbs enthalpy models. The latter is the emphasis of this work. Excess Gibbs enthalpy models are used to describe mixture equilibria. Regarding chemical engineering, they are central for the design and optimization of production processes.

The earliest models with nearest neighbor interactions are those using independent pair approximation. These models assume that all pairs of sites, and therefore all nearest neighbor contacts, are independent of each other. One of these models is the quasi-chemical method developed by Guggenheim [3], which is the basis of all activity coefficient models. This solution is only exact for the one-dimensional case with a coordination number of two. For higher coordination numbers the quasi-chemical method shows an increasing deviation from Monte Carlo simulations. This is due the approximate character of the degeneracy function for coordination numbers larger than two. [10]

The necessity of a higher accuracy than the independent pair approximation methods can provide sprouted various more elaborate models. A popular one of these is the cluster variation method, first introduced by Kikuchi in 1951. [6] Since then this method has been improved and expanded by Kikuchi and others. [8, 15] The predominant application is the traditional one, which is the creation of phase diagrams of alloys. However, the application of this method is currently expanding into new areas. [11]

The cluster variation method works by minimizing the Helmholtz free energy. The Helmholtz free energy can be expressed in terms of internal energy and entropy. For the internal energy, an exact expression can be found. The entropy term is usually modeled via an approximation. It should be noted that special cases exist where the cluster variation method results in an exact model rather than an approximation. The entropy is approximated by a truncated cumulant expansion. [11] A significant cluster is chosen and all possible subclusters including the original one are associated with a term in the entropy formula. It is assumed that all clusters that are bigger than the chosen one have a neglectable contribution to the entropy. [6]

The Helmholtz free energy is minimized with constraints. These constraints are general stochastic conditions, like the law of total probability or the Bayes theorem, that link the different clusters together. [6] This set of nonlinear equations is typically

solved numerically. For moderately sized clusters an algorithm was created by Kikuchi (the so called natural iteration method) which is designed to handle the large number of variables that arise from this system of equations. [7] For large clusters, like the 4x4x2 cluster considered by Pelizzola in 2014, the natural iteration method requires too much computational effort so that new algorithms have to be developed. The 4x4x2 cluster is the largest that is currently known. [12]

There are two main problems one has to solve when applying the cluster variation method. One is finding adequate approximations for the entropy as the number of expressions needed for this increases rapidly with the cluster size. The other problem is the minimization of the free energy regarding the large number of variables. The resulting long computation times are unsuitable for activity coefficient models. [2]

Because of these challenges of the cluster variation method Vinograd developed a different model which is based on the sequential construction of the lattice. The calculation is based on Markov chain theory and models the entropy using the information of a message defined by Shannon in the field of communication theory. [16]

This work explores the applications, expandability, and limitations of the Vinograd approach and proposes a model for the simple cubic lattice (coordination number of six) based on the same approach. The intention behind the derivation of this model is to provide a better foundation for activity coefficient models on the level of spherical molecules. The results are compared with the quasi-chemical method and data from Monte Carlo simulations.

2. General

2.1. Stochastic Basics and Nomenclature

The following nomenclature is introduced in order to shorten mathematical definitions and increase the readability of the equations in this work. In the case of a binary mixture each site in the lattice can be of type 1 or 2. In order to express the probability of a certain site to be of a specific type the following will be written: The probability of site A to be of type a is

$$p_a = Pr[A = a]. \quad (2-1)$$

The uppercase letters denote the position of the site within the lattice, while the lowercase letters describe the type of the molecule at that position. The combined probability of a group of sites, a so called cluster, is expressed by chaining the types with centered dots.

$$p_{a \cdot b \cdot c} = Pr[A = a \wedge B = b \wedge C = c] \quad (2-2)$$

Expressed in plain text both sides in equation (2-2) represent the probability of site A to be of type a and site B to be of type b and site C to be of type c .

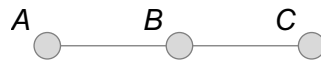


Figure 2-1.: $a \cdot b \cdot c$ cluster

Figure 2-1 shows an $a \cdot b \cdot c$ cluster in a chain configuration.

Conditional probabilities

In order to describe nearest neighbor interactions conditional probabilities are required. The probability that the site A is of type a given that site B is of type b is defined as

$$p_{a|b} = Pr[A = a|B = b] = \frac{Pr[A = a \wedge B = b]}{Pr[B = b]} = \frac{p_{a \cdot b}}{p_b}. \quad (2-3)$$

[5]

Various combinations of cluster and conditional probabilities are possible. One example is that the site A is dependent on the sites B and C .

$$p_{a|b \cdot c} = Pr[A = a|B = b \wedge C = c] = \frac{Pr[A = a \wedge B = b \wedge C = c]}{Pr[B = b \wedge C = c]} = \frac{p_{a \cdot b \cdot c}}{p_{b \cdot c}} \quad (2-4)$$

The insertion of a further conditional probability can be written similar to the definition of the conditional probability.

$$p_{a \cdot b|c} = p_{a|b \cdot c} \cdot p_{b|c} \quad (2-5)$$

Equation (2-5) shows that the probability of the $a \cdot b$ cluster dependent on c can be calculated from the probability of a dependent on the $b \cdot c$ cluster times the probability of b dependent on c .

Another important theorem when dealing with conditional probabilities is the law of total probability. Applied to cluster probabilities it means that the sum over all possible states of a site yields the probability of the cluster without that site. For the case of a simple two site cluster this means that the sum over all states of b of the $a \cdot b$ cluster results in the probability of a :

$$p_a = \sum_b p_{a|b} \cdot p_b = \sum_b p_{a \cdot b} \quad (2-6)$$

Again a dependency on c can be inserted which yields

$$p_{a|c} = \sum_b p_{a|b \cdot c} \cdot p_{b|c} = \sum_b p_{a \cdot b|c} \quad (2-7)$$

[1]

2.2. Thermodynamic Basics

This section is dedicated to giving definitions and general relations of basic thermodynamic variables used in this work. Most of the definitions and derivations are taken from Pielen. [14] The system considered is a binary mixture of molecules in a lattice arrangement with a constant coordination number z . N_1 is the number of molecules of component 1 and N_2 is the number of molecules of component 2. N is the total number of molecules in the system and defined as:

$$N = N_1 + N_2 \quad (2-8)$$

The global composition is introduced in order to move from the extensive numbers of molecules to intensive variables.

$$\begin{aligned} x_1 &= N_1/N \\ x_2 &= N_2/N \end{aligned} \quad (2-9)$$

The energetic interactions of the molecules are described by the contact between a pair of molecules, because nearest neighbor interactions are considered exclusively. N_{ij} is the number of contacts between molecules of type i and molecules of type j . The relations between the numbers of contacts is given by:

$$\begin{aligned} zN_1 &= 2N_{11} + N_{12} \\ zN_2 &= 2N_{22} + N_{21} \\ N_{12} &= N_{21} \end{aligned} \tag{2-10}$$

The energies of the contacts are given by ε_{11} , ε_{22} , and ε_{12} . It is convenient to define an exchange energy:

$$\omega = \omega_{12} = \varepsilon_{12} + \varepsilon_{21} - \varepsilon_{11} - \varepsilon_{22} \tag{2-11}$$

The local composition is an intensive analog to the number of contact pairs and is defined as:

$$\begin{aligned} x_{11} &= \frac{N_{11}}{zN_1} \\ x_{22} &= \frac{N_{22}}{zN_2} \\ x_{12} &= \frac{N_{12}}{zN_2} \\ x_{21} &= \frac{N_{21}}{zN_1} \end{aligned} \tag{2-12}$$

The local composition x_{ij} is the relative frequency of molecule type i next to molecule type j . From these definitions several correlations between the local compositions can be extracted.

$$\begin{aligned} \sum_i x_{ij} &= 1 \\ x_j x_{ij} &= x_i x_{ji} \end{aligned} \tag{2-13}$$

2.2.1. Quasi-chemical Approximation

The model proposed by Guggenheim is referred to as quasi-chemical because the exchange of one molecule of the considered contact pair is modeled similar to a chemical equilibrium reaction, as illustrated in figure 2-2.

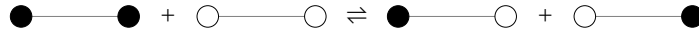


Figure 2-2.: Quasi-chemical equilibrium reaction

For this equilibrium reaction Guggenheim formulated the following expression:

$$N_{12}^2 = 4N_{11}N_{22} \exp\left(-\frac{\omega}{k_B T}\right) \quad (2-14)$$

On the basis of equation (2-14) the internal energy and the entropy can be formulated. For this, two auxiliary variables are introduced.

$$\eta = \exp\left(\frac{\omega}{2k_B T}\right) \quad (2-15)$$

$$\beta = \sqrt{1 + 4x_1x_2(\eta^2 - 1)}$$

The internal energy and entropy equations of the quasi-chemical approximation using β yield:

$$U = N \frac{z}{2} \left(x_1 \varepsilon_{11} + x_2 \varepsilon_{22} + x_1 x_2 \frac{\omega}{\beta + 1} \right)$$

$$S = -Nk_B \left(x_1 \ln x_1 + x_2 \ln x_2 - \frac{x_1 x_2 z \omega}{k_B T (\beta + 1)} \right. \quad (2-16)$$

$$\left. + \frac{z}{2} \left(x_1 \ln \frac{2x_1 + \beta - 1}{x_1 (\beta + 1)} + x_2 \ln \frac{-2x_1 + \beta - 1}{x_2 (\beta + 1)} \right) \right)$$

For a detailed derivation of the quasi-chemical theory in German, the work of Pielen [14] can be recommended. For an English version, the original publications of Guggenheim [3, 4] can be referred to.

2.3. Thermodynamic Consistency

One of the methods used to validate the thermodynamic consistency of the models analysed in this work is via a Gibbs-Helmholtz correlation. Gibbs-Helmholtz correlations are derived from the fundamental equations of thermodynamics and exist in different forms. The form used here is taken from Pfennig [13] and is as follows:

$$\left(\frac{\partial A}{\partial T} \right)_{V, x_i} = -\frac{U}{T^2} \quad (2-17)$$

The symbol A in equation (2-17) denotes the Helmholtz free energy, T is the absolute temperature, U is the internal energy, V is the volume and x_i is the global composi-

tion. Equation (2-17) states that the partial derivative of the free energy divided by temperature with respect to the temperature and constant volume and composition equals the negative internal energy divided by the squared temperature.

The consistency check is performed numerically because the models have no explicit solutions. For this the partial derivative is approximated using the quotient of differences. For a constant value of the global composition and the interaction energies, the temperature is varied in steps of about half the precision of the working precision of the equation solving algorithm. The models are solved for these temperatures and the free energy and the internal energy are determined. For the left hand side the differences that approximate the derivative are formed. In order to calculate the right hand side of equation (2-17) the mean of the two values is formed. The difference of the two sides of the equation is then tested for equality with zero.

$$\left(\frac{\frac{A_{j+1}}{T_{j+1}} - \frac{A_j}{T_j}}{T_{j+1} - T_j} \right) + \frac{2(U_{j+1} + U_j)}{(T_{j+1} + T_j)^2} = 0 \quad (2-18)$$

2.4. Monte Carlo Simulations

Throughout this work, the developed models are compared to data from Monte Carlo simulations. These simulations are based on the work of Lisa König and were modified to output the probabilities of clusters. [9] Monte Carlo simulations are considered for comparison because they give the most accurate representation of the initial lattice assumptions. A hypothetical simulation of an infinite lattice with infinitely many steps would accurately describe the regular mixture with the given assumptions. The lattice size and number of steps are chosen as a compromise between precision and computation time.

The simulations work by constantly exchanging two neighboring molecules. The energetic state of the lattice before and after the exchange are evaluated and compared. If the exchange is energetically favorable it is performed. If the energy of the lattice increases because of this exchange it has a random chance of occurrence. This random chance is dependent on the magnitude of the increase of energy. The bigger the increase of energy in the lattice is, the smaller is the chance of the exchange occurring.

The simulations yield information about the local composition as well as the internal energy of the lattice in equilibrium. The entropy of the lattice is calculated from the internal energy using a Gibbs-Helmholtz integration.

2.5. Model Development using Wolfram Mathematica

During the development of the models, all calculations were executed using Wolfram Mathematica in the versions 10.3 and 11.0. [18, 19]

2.5.1. Applications and Packages

A few applications and packages were developed to extend the Wolfram Language with functions that simplify the manipulation of systems of equations containing probabilities. Some of the key features are presented in this section.

The main Mathematica application developed in this work is named "MasterThesis-Mayer". The application's containing functions focus on creating and manipulating symbolic expressions with lattice probabilities as variables. At the center of this is the function `P` which creates probability symbols based on their indices and thus allows the use of iterators during the creation of symbols. The functions `PTable` and `PSum` are versions of the built in functions `Table` and `Sum` that are designed to work well with the function `P` in the context of lattice systems. This application also includes functions for graphical representations of lattice systems and shortcuts for working with logarithms and applying the Lagrange optimization method. Some intermediate results, graphics and descriptions thereof are collected in a database which can be accessed through the package "MasterThesisMayerDatabase".

The application "FormattedOutput" was created for styling the notebooks and presenting the calculation results. A noteworthy function of this application is `DeviationView` which calculates the relative deviations of lists of data and displays the result in a grid. This function is used in most notebooks to compare different models to each other and to Monte Carlo data.

More information about these applications can be found in their documentation which can be accessed through the Mathematica documentation center once the applications are loaded.

The resulting models together with the quasi-chemical approximation and some Monte Carlo data are combined into the package "NumericalModelSolutions". All numerical model functions are structured the same. As arguments they expect the global composition of molecule type 1 x_1 , the dimensionless exchange energy $\omega/k_B T$, the dimensionless interaction energy of component 1 with itself $\varepsilon_{11}/k_B T$, and the dimensionless interaction energy of component 2 with itself $\varepsilon_{22}/k_B T$. The output of these functions is in form of an `Association`, which is the Wolfram Language's

implementation of key and value pairs. The six lists of entries in this `Association` are the conditional pair probabilities, the cluster probabilities, the conditional probabilities, the neighborhood probabilities, the internal energy, and the entropy for the respective model. The identical structure of input and output of all model functions allows a relatively simple automation of tests and comparisons to be performed with the models.

2.5.2. Manipulation of Systems of Equations

Wolfram Mathematica lends itself nicely towards working with symbolic expressions. One very important feature for manipulating symbolic expressions is `ReplaceAll` together with rules. A `Rule` connects two expressions together and with `ReplaceAll` these rules can be applied to change part of an expression according to these rules. Working with rules allows for more flexibility and reusability of code compared to assigning each subexpression to a variable. Even Mathematica's output of equation solving algorithms is in the form of lists of rules.

Simplifying or restructuring expressions can be achieved with functions like `Simplify`, `Cancel`, and `Collect`. These functions are very powerful and are only limited by the available computational performance and system memory. They also allow the definition of `Assumptions` which can aid the simplifications. One example would be to limit the probabilities to a range between zero and one.

The function `Solve` is used for symbolic solutions of equations. For numerical evaluations the functions `FindRoot` and `FindMinimum` were used, because they allow for a higher complexity and size of the system of equations than their alternatives `NSolve` and `NMinimize`. The numerical precision of these algorithms can easily be set with the option `WorkingPrecision`.

3. Chain Lattice (1D)

This chapter contains the one-dimensional approach developed by Vinograd. [16] For the one-dimensional case, a lattice in the shape of a chain is constructed. This chain shall contain a sufficiently large number of molecules (N) so that boundary effects are neglectable. In the following paragraphs, the addition of site A to the end of the chain is considered, as illustrated in figure 3-1.



Figure 3-1.: 1D chain construction - addition of site A to the end of the chain

Since nearest neighbor interactions are considered exclusively, the insertion process of site A is only dependent on the previously placed site B . The probability of site A being of type a dependent on site B being of type b ($p_{a|b}$) forms the transition matrix of the discrete Markov process.

$$\begin{array}{c|cc} & 1 & 2 \\ \hline 1 & p_{1|1} & p_{2|1} \\ 2 & p_{1|2} & p_{2|2} \end{array} \quad (3-1)$$

The application of the law of total probability to the transition probabilities results in the expressions

$$\begin{aligned} p_{1|1} + p_{2|1} &= 1 \\ p_{1|2} + p_{2|2} &= 1. \end{aligned} \quad (3-2)$$

This Markov chain is ergodic except for a special case ($p_{1|1} = 1, p_{2|2} = 0$). This means that the probabilities of a certain site to be of type 1 or 2 (p_1, p_2) take on constant values after an infinite amount of steps. These values equal the global composition of the mixture:

$$\begin{aligned} p_1 &= x_1 \\ p_2 &= x_2 \end{aligned} \quad (3-3)$$

The law of total probability can also be applied over a column in the transition matrix:

$$p_1 p_{1|1} + p_2 p_{1|2} = p_1 \quad (3-4)$$

Replacing $p_{1|1}$ with expression (3-2) yields

$$p_1 p_{2|1} = p_2 p_{1|2} \quad (3-5)$$

which can be interpreted as a condition of symmetry. It states that the probability of a molecule 1 being next to a molecule 2 is the same as the probability of a molecule 2 being next to a molecule 1. Expressed with cluster probabilities this can be written as

$$p_{1 \cdot 2} = p_{2 \cdot 1} \quad (3-6)$$

Equation (3-5) together with equations (3-2) reduces the number of independent transition probabilities to one, i.e. $p_{1|2}$. In order to calculate this last probability, the equilibrium state has to be considered. Similar to many other models in statistical thermodynamics, the equilibrium is achieved via the minimization of the Helmholtz free energy at a given temperature. The Helmholtz free energy can be expressed using the internal energy and the entropy.

$$A = U - TS \quad (3-7)$$

The internal energy for nearest neighbor interactions is calculated by adding up the interaction energies of all molecule pairs in the lattice. In terms of probabilities, this is equal to the sum of all interaction energies weighted with each respective pair probability and multiplied by the total number of molecules.

$$U = N \sum_b p_b \sum_a p_{a|b} \varepsilon_{ab} \quad (3-8)$$

After applying the sums the energy equation results in

$$U = N (p_1 (p_{1|1} \varepsilon_{11} + p_{2|1} \varepsilon_{12}) + p_2 (p_{1|2} \varepsilon_{21} + p_{2|2} \varepsilon_{22})) \quad (3-9)$$

This equation can be rewritten using ω as defined in equation (2-11) and afterwards simplified by considering the correlations in equations (3-2) and (3-5):

$$U = N (p_1 \varepsilon_{11} + p_2 \varepsilon_{22} + p_2 p_{1|2} \omega) \quad (3-10)$$

The entropy of this lattice is modeled by applying concepts of communication theory. In this field, Shannon defined the information of a message as a function of the

probability of an event. This information can be used to develop an expression for the entropy. In case of the one-dimensional lattice, this expression is

$$S = -Nk_B \sum_b p_b \sum_a p_{a|b} \ln(p_{a|b}). \quad (3-11)$$

3.1. Minimization of the Helmholtz free energy

Since the number of molecules and the temperature are constant it is convenient to minimize the dimensionless free energy.

$$\frac{A}{k_B N T} = \min \quad (3-12)$$

Inserting the expressions for entropy (equation (3-11)) and internal energy (equation (3-10)) into equation (3-7) yields

$$\begin{aligned} A = N & (p_1 \varepsilon_{11} + p_2 \varepsilon_{22} + p_2 p_{1|2} \omega) \\ & + TNk_B (p_1 p_{1|1} \ln(p_{1|1}) + p_1 p_{2|1} \ln(p_{2|1}) + p_2 p_{1|2} \ln(p_{1|2}) + p_2 p_{2|2} \ln(p_{2|2})). \end{aligned} \quad (3-13)$$

Bringing equation (3-13) into the dimensionless form results in

$$\begin{aligned} \frac{A}{k_B N T} = p_1 & \frac{\varepsilon_{11}}{k_B T} + p_2 \frac{\varepsilon_{22}}{k_B T} + p_2 p_{1|2} \frac{\omega}{k_B T} \\ & + p_1 p_{1|1} \ln(p_{1|1}) + p_1 p_{2|1} \ln(p_{2|1}) + p_2 p_{1|2} \ln(p_{1|2}) + p_2 p_{2|2} \ln(p_{2|2}). \end{aligned} \quad (3-14)$$

For the minimization of equation (3-14) equations (3-2) and (3-5) have to be included as constraints in order to correctly account for the dependencies between the transitional probabilities:

$$\begin{aligned} p_{1|1} + p_{2|1} &= 1 \\ p_{1|2} + p_{2|2} &= 1 \\ p_1 p_{2|1} - p_2 p_{1|2} &= 0 \end{aligned} \quad (3-15)$$

The constrained minimization is executed by using the Lagrange method. The resulting Lagrange function takes on the form of

$$\begin{aligned}
\mathcal{L} = & p_1 \frac{\varepsilon_{11}}{k_B T} + p_2 \frac{\varepsilon_{22}}{k_B T} + p_2 p_{1|2} \frac{\omega}{k_B T} \\
& + p_1 p_{1|1} \ln(p_{1|1}) + p_1 p_{2|1} \ln(p_{2|1}) + p_2 p_{1|2} \ln(p_{1|2}) + p_2 p_{2|2} \ln(p_{2|2}) \\
& - \lambda_1 (p_{1|1} + p_{2|1} - 1) \\
& - \lambda_2 (p_{1|2} + p_{2|2} - 1) \\
& - \lambda_3 (p_1 p_{2|1} - p_2 p_{1|2})
\end{aligned} \tag{3-16}$$

where the lambdas represent the Lagrangian multipliers. The Lagrangian multipliers connect the target function with the constraints. They are independent from the transitional probabilities. [17] The partial derivatives of the Lagrange function with respect to the transitional probabilities are set to zero as the necessary condition of the minimum at the equilibrium point.

$$\begin{aligned}
\frac{\partial \mathcal{L}}{\partial p_{1|1}} = 0 &= p_1 - \lambda_1 + p_1 \ln(p_{1|1}) \\
\frac{\partial \mathcal{L}}{\partial p_{2|1}} = 0 &= p_1 - \lambda_1 - p_1 \lambda_3 + p_1 \ln(p_{2|1}) \\
\frac{\partial \mathcal{L}}{\partial p_{1|2}} = 0 &= p_2 - \lambda_2 + p_2 \lambda_3 + p_2 \frac{\omega}{k_B T} + p_2 \ln(p_{1|2}) \\
\frac{\partial \mathcal{L}}{\partial p_{2|2}} = 0 &= p_2 - \lambda_2 + p_2 \ln(p_{2|2})
\end{aligned} \tag{3-17}$$

Eliminating the three lambdas from this set of equations yields

$$\exp\left(\frac{\omega}{k_B T}\right) = \frac{p_{1|1} p_{2|2}}{p_{1|2} p_{2|1}}. \tag{3-18}$$

The equation (3-18) together with the constraints (equation (3-15)) can be solved with regard to the transitional probabilities.

$$\begin{aligned}
 p_{1|1} &= 1 - \frac{2p_2}{1 + \sqrt{1 + 4(\exp(\frac{\omega}{k_B T}) - 1)p_1 p_2}} \\
 p_{2|1} &= \frac{2p_2}{1 + \sqrt{1 + 4(\exp(\frac{\omega}{k_B T}) - 1)p_1 p_2}} \\
 p_{1|2} &= \frac{2p_1}{1 + \sqrt{1 + 4(\exp(\frac{\omega}{k_B T}) - 1)p_1 p_2}} \\
 p_{2|2} &= 1 - \frac{2p_1}{1 + \sqrt{1 + 4(\exp(\frac{\omega}{k_B T}) - 1)p_1 p_2}}
 \end{aligned} \tag{3-19}$$

Equation (3-19) gives the solution for the one-dimensional case. It should be noted, that the one-dimensional lattice is the only case where an explicit solution of Vinograd's approach is possible. The systems of equations for the higher dimensional cases must, therefore, be solved numerically.

3.2. Comparison to Guggenheim

For the one-dimensional chain lattice, the exclusive consideration of nearest neighbor interactions leads to the equality of Vinograd's approach and Guggenheim's quasi-chemical theory. This relation is important because the quasi-chemical theory is an exact solution of the simple chain lattice. However, the degeneracy function of the quasi-chemical theory is only exact for the one-dimensional chain. The approximations of higher dimensions using this degeneracy function are rather crude, which leads to the necessity of alternative models. [10]

4. Square Lattice (2D)

The two-dimensional square lattice is constructed, in terms of Markov chains, similarly to the one-dimensional chain. This construction of the square lattice is proposed by Vinograd. [16] Again, the addition of site *A* is considered in order to illustrate the sequential construction procedure. This addition procedure is depicted in figure 4-1.

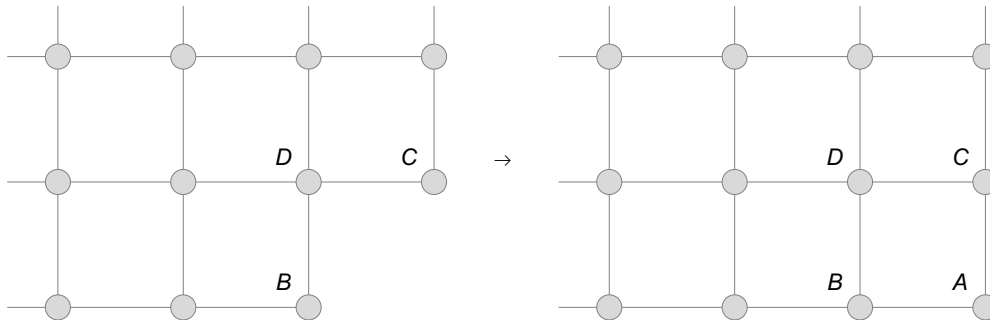


Figure 4-1.: 2D square lattice construction - addition of site *A* to the lattice

Each row of the lattice is filled with molecules from left to right. After a row is completed, the next row below it is started. This one is also filled from left to right. This lattice is, similar to the one-dimensional case, large enough so that boundary effects are neglectable. Therefore the further considerations are based on an infinitely large lattice. Because of the exclusive consideration of nearest neighbor interactions, the addition of site *A* is only dependent on the sites *B* and *C*. What may at first seem a bit counterintuitive is the fact that the insertion of site *B* is independent of the insertion of site *C*. All site additions are only dependent on the sites directly above and left of them. This means that the sites *B* and *C* are both dependent on site *D*, but not on one another. In fact, the additions of sites *B* and *C* are separated by an infinite number of steps.

With this construction in mind, the entropy of the two-dimensional square lattice can be modeled as

$$S = -Nk_B \sum_{b,c} p_{b \cdot c} \sum_a p_{a|b \cdot c} \ln(p_{a|b \cdot c}) \quad (4-1)$$

In equation (4-1), $p_{b \cdot c}$ is the probability of the neighborhood that site *A* is placed into. The probability of the insertion process is $p_{a|b \cdot c}$.

The internal energy is again modeled as the sum of all contact pairs weighted with each respective probability of occurrence.

$$U = N \sum_{b,c} p_{b \cdot c} \sum_a p_{a|b \cdot c} (\varepsilon_{ab} + \varepsilon_{ac}) \quad (4-2)$$

This expression can be rewritten with cluster probabilities by applying the stochastic rules defined in section 2.1. The neighborhood probability multiplied with the probability of the A insertion yields the cluster probability of the sites A , B and C which contains both contact pairs.

$$p_{a \cdot b \cdot c} = p_{b \cdot c} p_{a|b \cdot c} \quad (4-3)$$

Applied to the internal energy this gives

$$U = N \sum_{a,b,c} p_{a \cdot b \cdot c} (\varepsilon_{ab} + \varepsilon_{ac}). \quad (4-4)$$

The equation for the entropy can also be rewritten with cluster probabilities. Besides the correlation between the cluster probabilities ($p_{a \cdot b \cdot c}$), the neighborhood probabilities ($p_{b \cdot c}$) and the conditional probabilities ($p_{a|b \cdot c}$) given in equation (4-3), also the calculation of the neighborhood probabilities from the cluster probabilities is required. This correlation can be found by applying the law of total probability. The summation of the cluster probabilities over all possible states of a yields the neighborhood probabilities.

$$p_{b \cdot c} = \sum_a p_{a \cdot b \cdot c} \quad (4-5)$$

The application of equations (4-3) and (4-5) to equation (4-1) results in the entropy expressed with the probabilities of the $a \cdot b \cdot c$ cluster.

$$S = -Nk_B \sum_{a,b,c} p_{a \cdot b \cdot c} \ln \left(\frac{p_{a \cdot b \cdot c}}{\sum_a p_{a \cdot b \cdot c}} \right) \quad (4-6)$$

Because of these connections between the cluster probabilities and the conditional probabilities, it is inherent that both can be used interchangeably.

All two-dimensional models are solved with a numerical minimization of the Helmholtz free energy under consideration of the approximation of the cluster probabilities using pair probabilities that each model provides and with the dependencies between the pair probabilities, which are given in equation (3-15). The Lagrange method for solving

the system of equations has also been tested. The result of this investigation is the realization that no explicit solution for the models is possible. This method requires a higher computational effort than a minimization. Therefore, it is recommended that the equations are solved by applying a numerical minimization. Multiple models for approximating the cluster probabilities are presented in the following sections.

4.1. Vinograd's First Approximation

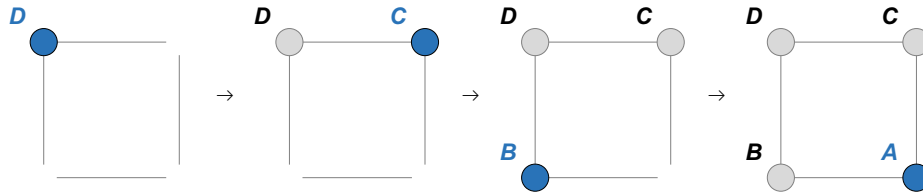


Figure 4-2.: 2D Vinograd's first approximation lattice construction

This section deals with the derivation of Vinograd's first approximation. [16] The construction of the considered cluster is illustrated in figure 4-2. The first approximation proposed by Vinograd treats the cluster formed by the sites B , C and D like a one-dimensional chain. Site D is the starting point. Sites B and C are each placed dependent on site D . They are, however, independent from one another. Therefore the starting point of this chain, as well as its construction direction, do not matter.

$$\rho_{b \cdot c \cdot d} = \rho_d \rho_{c|d} \rho_{b|d} = \rho_b \rho_{d|b} \rho_{c|d} = \rho_c \rho_{d|c} \rho_{b|d} \quad (4-7)$$

The probability of the $b \cdot c \cdot d$ cluster can be used to calculate the probability of the $b \cdot c$ cluster. This happens via a summation over all possible paths that lead to this cluster. In this case, it means the summation over all possible states of d , which are two for a binary system. The resulting cluster represents the neighborhood in which the molecule a is to be placed.

$$\rho_{b \cdot c} = \sum_d \rho_{b \cdot c \cdot d} = \sum_d \rho_d \rho_{c|d} \rho_{b|d} \quad (4-8)$$

Together with equation (4-3), which shows the insertion of molecule a into this neighborhood, it yields

$$\rho_{a|b \cdot c} = \rho_{a \cdot b \cdot c} / \sum_d \rho_{b \cdot c \cdot d} \quad (4-9)$$

The following correlation can be found because the sum of all options for the addition of molecule a must equal one.

$$\sum_a \rho_{a|b \cdot c} = 1 = \sum_a \rho_{a \cdot b \cdot c} / \sum_d \rho_{b \cdot c \cdot d} \quad (4-10)$$

From equation (4-10) Vinograd deduces that the probability of the $a \cdot b \cdot c$ cluster is given by

$$p_{a \cdot b \cdot c} = p_a p_{b|a} p_{c|a \cdot b} \quad (4-11)$$

$p_{1 \cdot 1 \cdot 1} = p_1 p_{1 1}^2$	
$p_{1 \cdot 1 \cdot 2} = p_1 p_{1 1} p_{2 1}$	
$p_{1 \cdot 2 \cdot 1} = p_1 p_{1 1} p_{2 1}$	
$p_{1 \cdot 2 \cdot 2} = p_1 p_{2 1}^2$	
$p_{2 \cdot 1 \cdot 1} = p_2 p_{1 2}^2$	
$p_{2 \cdot 1 \cdot 2} = p_2 p_{1 2} p_{2 2}$	
$p_{2 \cdot 2 \cdot 1} = p_2 p_{1 2} p_{2 2}$	
$p_{2 \cdot 2 \cdot 2} = p_2 p_{2 2}^2$	

Table 4-1.: 2D first approximation: cluster probabilities

Table 4-1 lists all eight cluster probabilities $p_{a \cdot b \cdot c}$ and their respective approximations. In the lattice graphics, molecules of type 1 are represented by black disks and molecules of type 2 by white disks.

Resulting System of Equations

The system in equilibrium is calculated by minimizing the Helmholtz free energy. Inserting the expressions for the internal energy and the entropy given at equations (4-4) and (4-6) into equation (3-7) yields the target function for the minimization.

$$\frac{A}{k_B N T} = \sum_{a,b,c} p_{a \cdot b \cdot c} \left(\frac{\varepsilon_{ab}}{k_B T} + \frac{\varepsilon_{ac}}{k_B T} + \ln \left(\frac{p_{a \cdot b \cdot c}}{\sum_a p_{a \cdot b \cdot c}} \right) \right) \quad (4-12)$$

The constraints of this optimization are the equations that connect the eight cluster probabilities $p_{a \cdot b \cdot c}$ to the four conditional pair probabilities $p_{a|b}$ given by formula (4-11).

$$p_{a \cdot b \cdot c} = p_a p_{b|a} p_{c|a} \quad (4-13)$$

The formula (4-13) describes 8 equations where the iterators a , b and c each take on the states 1 and 2. Also, the correlations between the conditional pair probabilities are needed. It is recommended to express three of the conditional pair probabilities as a function of the fourth, in order to reduce the number of variables. The formulas that are given by equation (3-15) are therefore transformed into the following form.

$$\begin{aligned} p_{1|1} &= 1 - \frac{p_{1|2} p_2}{p_1} \\ p_{2|2} &= 1 - p_{1|2} \\ p_{2|1} &= \frac{p_{1|2} p_2}{p_1} \end{aligned} \quad (4-14)$$

The resulting system of equations consists of 12 equations and 13 variables which are the free energy A , the 4 conditional pair probabilities p_{ij} and the 8 cluster probabilities $p_{a \cdot b \cdot c}$. The equations (4-13) and (4-14) can be inserted into equation (4-12) which would yield one single equation dependent on one variable ($p_{1|2}$). This equation, however, can only be minimized numerically. Due to the size of the resulting equation it is in general recommended to work with the system of equations and constrained minimization instead.

4.1.1. Comparison to Guggenheim and Monte Carlo Simulations

Vinograd's first approximation is compared to Monte Carlo simulation results in order to assess the quality of this model. Guggenheim's quasi-chemical approach is used as a reference model.

The figures 4-3 and 4-4 show the relative deviation of Vinograd's first approximation and Guggenheim's quasi-chemical theory to the Monte Carlo simulation results. Figure 4-3 depicts the relative deviation of the internal energy and figure 4-4 shows the relative deviation of the entropy. The relative deviation is calculated by subtracting

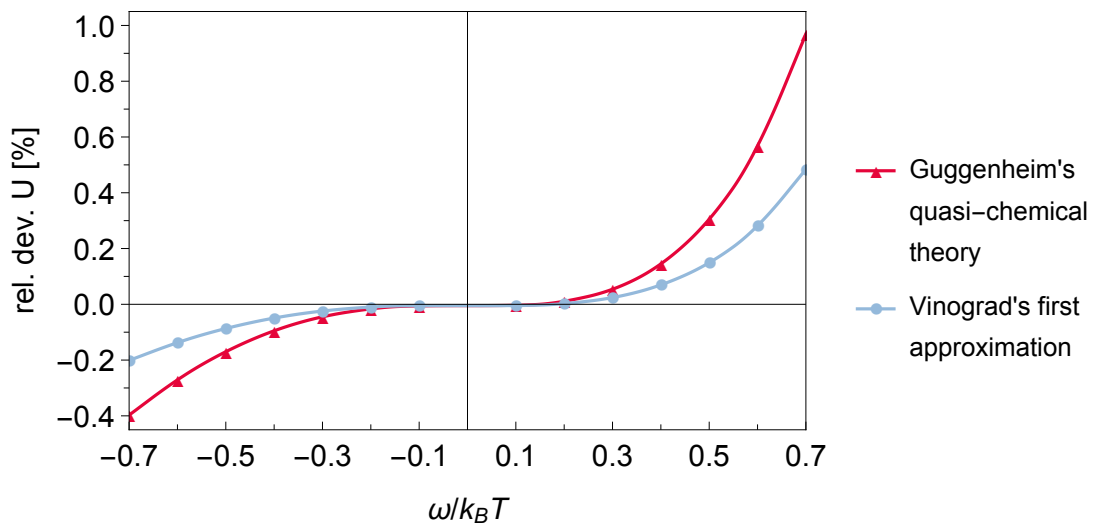


Figure 4-3.: Comparison of Vinograd's first approximation with MC-Simulations and Guggenheim: Internal Energy ($p_1 = 0.3, \varepsilon_{11} = \varepsilon_{22} = 0$, rel. dev. = $((\text{model} - \text{simulation}) / \text{simulation}) 100\%$)

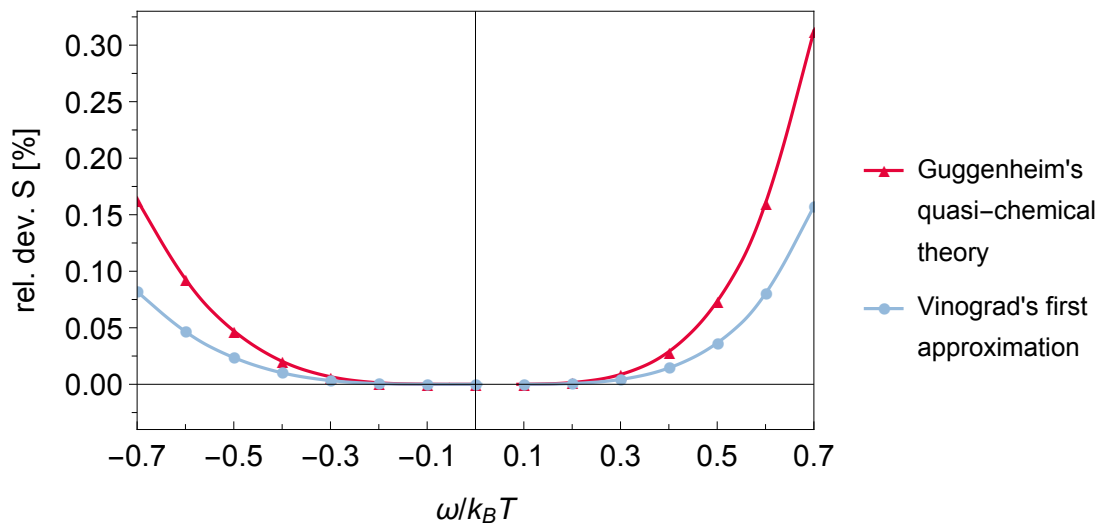


Figure 4-4.: Comparison of Vinograd's first approximation with MC-Simulations and Guggenheim: Entropy ($p_1 = 0.3, \varepsilon_{11} = \varepsilon_{22} = 0$, rel. dev. = $((\text{model} - \text{simulation}) / \text{simulation}) 100\%$)

the Monte Carlo simulation data from the model solution and dividing this by the simulation data.

$$\text{relative deviation} = \frac{\text{model} - \text{simulation}}{\text{simulation}} 100\% \quad (4-15)$$

The deviations are evaluated at different dimensionless interaction energies with the global composition of molecule 1 being 0.3 and the interaction energies of the pure components set to zero. The interaction energies of the pure components do not

influence the equilibrium compositions. They only change the value of the internal energy.

In the case of the two-dimensional square lattice, the deviation of Vinograd's first approximation is roughly half of the deviation of Guggenheim's quasi-chemical theory. This means, that this first approximation already offers a considerable advantage compared to the quasi-chemical theory.

4.1.2. Thermodynamic Consistency Check

The model is not only compared with simulation results but also investigated regarding thermodynamic properties and correlations. Two different methods for testing the consistency are performed. The first is a numerical evaluation of a Gibbs-Helmholtz equation.

$$\left(\frac{\partial A}{\partial T} \right)_{V, x_i} = - \frac{U}{T^2} \quad (4-16)$$

Equation (4-16) checks the thermodynamic correlation between the internal energy and the Helmholtz free energy. Details of this procedure are given in section 2.3. The result of this validation is that Vinograd's first approximation fulfills the Gibbs-Helmholtz correlation.

The second consistency check is the analysis of boundary conditions. For this purpose, the ratio of the probability of a molecule being of type 1 with the condition that its neighbor is of type 2 to the global probability of the molecule being of type 1 is evaluated for different exchange energies. Figure 4-5 shows this ratio of $p_{1|2}/p_1$ which can also be expressed as the ratio of the local composition to the global composition x_{12}/x_1 . The abscissa marks the dimensionless exchange energy $\omega/k_B T$ where the negative values denote an attraction between the molecules of types 1 and 2 and the positive values denote a repulsion between the two. Each line in the figure represents one global composition. One important point is random mixing where there is no interaction between the molecules. No interaction results in the fact that all molecules are independent of each other which in turn leads to $p_{1|2}/p_1 = 1$. In figure 4-5 it is clearly visible that $p_{1|2}/p_1$ equals one for Vinograd's first approximation calculated with zero interaction. This means that this model perfectly describes the case of random mixing.

The next boundary which is considered is that of $\omega/k_B T$ approaching negative infinity. This state of maximum attraction yields a lattice where each molecule of the less

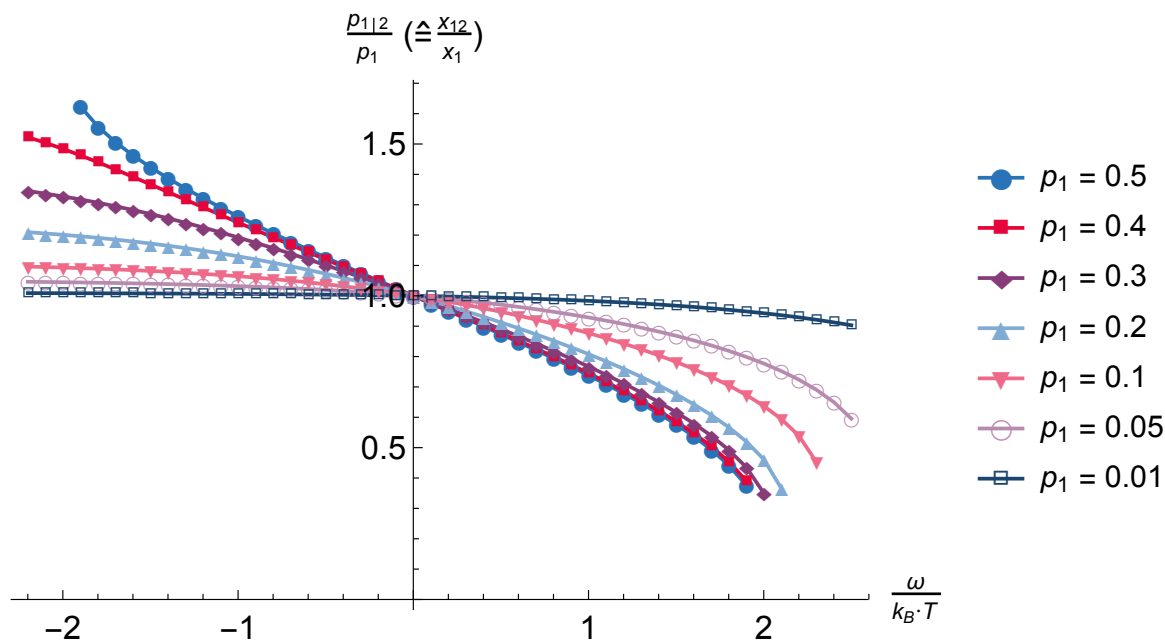


Figure 4-5.: 2D Vinograd's first approximation: $\frac{p_{1|2}}{p_1}$ over $\frac{\omega}{k_B T}$

frequent type 1 is completely surrounded by molecules of type 2. Therefore the value for $p_{1|1}$ approaches zero. Using the correlations between the conditional pair probabilities given by equation (3-15) the limit for $p_{1|2}/p_1$ can be calculated.

$$\lim_{\frac{\omega}{k_B T} \rightarrow -\infty} \frac{p_{1|2}}{p_1} = \frac{1}{p_2} \quad (4-17)$$

Figure 4-5 shows that even though the model approaches these limits, it does so quite slowly. This slow convergence is caused by the assumption of independence of the pairs of molecules, which is the basis of Vinograd's first approximation.

The boundary where $\omega/k_B T$ is approaching positive infinity cannot be described in a similar fashion because of the miscibility gap that occurs before the system converges. It should be noted that this model will not give solutions for separate phases in the miscibility gap. The reason for this is the fact that this model considers the lattice as a whole and therefore returns the probabilities averaged over all phases.

4.1.3. Asymmetry

The problem with this model, as Vinograd mentions, is that the sequential algorithm of lattice construction causes an asymmetry in next to nearest neighbor pairs. This means that the direction of lattice growth has an influence on the neighborhood probability and therefore the whole $a \cdot b \cdot c \cdot d$ cluster. To illustrate this, the square

cluster will be constructed in two different directions. One starting with site D , as was shown before and the other starting with site C .

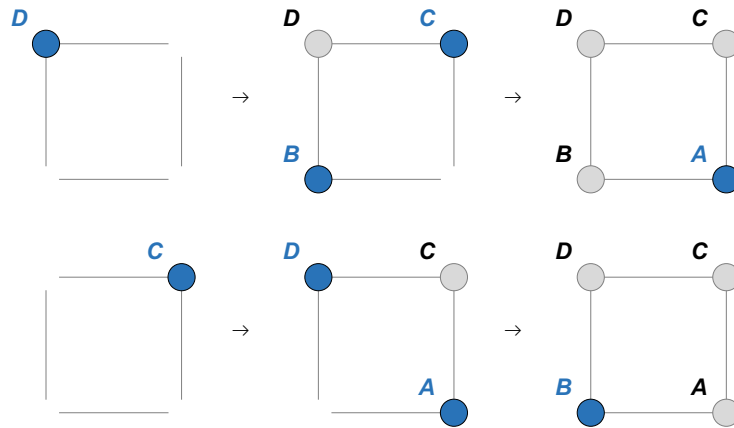


Figure 4-6.: Two construction directions for the 2D lattice

Figure 4-6 shows the two different construction directions. During the second step, the order in which the two molecules are placed is irrelevant. The reason for this is the fact that the two events are independent of one another.

$$\rho_{a \cdot b \cdot c \cdot d} = \rho_d \rho_{b|d} \rho_{c|d} \rho_{a|b \cdot c} \quad (4-18)$$

$$\rho_{a \cdot b \cdot c \cdot d} = \rho_c \rho_{a|c} \rho_{d|c} \rho_{b|a \cdot d}$$

The probability of the last insertion step can be calculated from equation (4-11):

$$\rho_{a|b \cdot c} = \frac{\rho_{a \cdot b \cdot c}}{\sum_a \rho_{a \cdot b \cdot c}} = \frac{\rho_a \rho_{b|a} \rho_{c|a}}{\sum_a \rho_a \rho_{b|a} \rho_{c|a}} \quad (4-19)$$

$$\rho_{b|a \cdot d} = \frac{\rho_{a \cdot b \cdot d}}{\sum_b \rho_{a \cdot b \cdot d}} = \frac{\rho_b \rho_{a|b} \rho_{d|b}}{\sum_b \rho_b \rho_{a|b} \rho_{d|b}}$$

Replacing the probability of each last insertion step in equations (4-18) with the expressions developed in equations (4-19) yields

$$\rho_{a \cdot b \cdot c \cdot d} = \frac{\rho_d \rho_{b|d} \rho_{c|d} \rho_a \rho_{b|a} \rho_{c|a}}{\sum_a \rho_a \rho_{b|a} \rho_{c|a}} \quad (4-20)$$

$$\rho_{a \cdot b \cdot c \cdot d} = \frac{\rho_c \rho_{a|c} \rho_{d|c} \rho_b \rho_{a|b} \rho_{d|b}}{\sum_b \rho_b \rho_{a|b} \rho_{d|b}}$$

The table 4-2 shows that this first approximation is asymmetric and therefore lacks a property which is expected from such a model.

4.2. Vinograd's Second Approximation

Vinograd proposes a second approximation in order to remedy the asymmetry that the first approximation contains. [16] The aim of this approximation is to keep the structure of the first approximation whilst making the cluster probabilities independent of the lattice growth direction. The proposed method of achieving this goal is by defining the probability of the square cluster $p_{a \cdot b \cdot c \cdot d}$ as the average over all possible lattice growth directions.

$$p_{a \cdot b \cdot c \cdot d} = \frac{1}{4} (p_{b \cdot c \cdot d} p_{a|b \cdot c} + p_{a \cdot c \cdot d} p_{b|a \cdot d} + p_{a \cdot b \cdot d} p_{c|a \cdot d} + p_{a \cdot b \cdot c} p_{d|b \cdot c}) \quad (4-21)$$

The different construction directions have a diagonal symmetry because of the structure of the equations. Therefore it is only necessary to calculate the mean of two directions.

$$p_{a \cdot b \cdot c \cdot d} = \frac{1}{2} (p_{b \cdot c \cdot d} p_{a|b \cdot c} + p_{a \cdot c \cdot d} p_{b|a \cdot d}) \quad (4-22)$$

Figure 4-7 depicts the two construction directions of the square cluster. The neighbor-

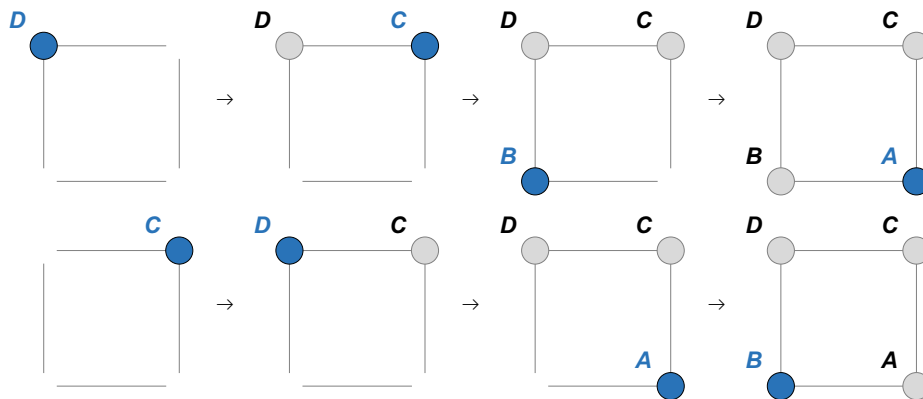


Figure 4-7.: 2D Vinograd's second approximation lattice construction

hood probabilities of the first direction are constructed by starting with site D . Then site C is placed which is dependent on site D . Site B is inserted depending on site D but not site C because they are not nearest neighbors and in the complete lattice, site C is placed infinitely many steps before site B .

$$p_{b \cdot c \cdot d} = p_d p_{c|d} p_{b|d} \quad (4-23)$$

The insertion of site A is dependent on the sites B and C and can be calculated with the expression developed in equation (4-19).

$$p_{a|b \cdot c} = \frac{p_a p_{b|a} p_{c|a}}{\sum_a p_a p_{b|a} p_{c|a}} \quad (4-24)$$

Inserting the equations (4-23) and (4-24) into equation (4-22) yields the correlation of the probabilities of the square cluster with the conditional pair probabilities according to Vinograd's second approximation.

$$p_{a \cdot b \cdot c \cdot d} = \frac{1}{2} \left(p_d p_{b|d} p_{c|d} \frac{p_a p_{b|a} p_{c|a}}{\sum_a p_a p_{b|a} p_{c|a}} + p_c p_{a|c} p_{d|c} \frac{p_b p_{a|b} p_{d|b}}{\sum_b p_b p_{a|b} p_{d|b}} \right) \quad (4-25)$$

The entropy and energy formulas have to be expanded, in order to accommodate the four site cluster probabilities. Regarding the entropy, this is achieved by taking equation (4-1) and adding the new fourth site to the outer sum.

$$S = -Nk_B \sum_{b,c,d} p_{b \cdot c \cdot d} \sum_a p_{a|b \cdot c \cdot d} \ln(p_{a|b \cdot c \cdot d}) \quad (4-26)$$

The conditional probabilities of the insertion of site A using the definition of conditional probabilities yields:

$$p_{a|b \cdot c \cdot d} = \frac{p_{a \cdot b \cdot c \cdot d}}{p_{b \cdot c \cdot d}} \quad (4-27)$$

The neighborhood probabilities can be calculated from the four site cluster probabilities by applying the law of total probability.

$$p_{b \cdot c \cdot d} = \sum_a p_{a \cdot b \cdot c \cdot d} \quad (4-28)$$

Substituting the conditional probabilities with equation (4-27) and the neighborhood probabilities with equation (4-28), the entropy with regard to the square cluster can be rewritten as:

$$S = -Nk_B \sum_{b,c,d} p_{a \cdot b \cdot c \cdot d} \ln \left(\frac{p_{a \cdot b \cdot c \cdot d}}{\sum_a p_{a \cdot b \cdot c \cdot d}} \right) \quad (4-29)$$

The equation for the internal energy can be modified similar to the entropy. Considering equation (4-4) as the basis, the adaptation consists again of replacing the probabilities and expanding the summation to incorporate the molecule d .

$$U = N \sum_{a,b,c,d} p_{a \cdot b \cdot c \cdot d} (\varepsilon_{ab} + \varepsilon_{ac}). \quad (4-30)$$

It is noteworthy to mention that even though the new cluster contains two additional contact pairs, $b \cdot d$ and $c \cdot d$, their interaction energies are not added to the equation. The reason is that equation (4-30) already sums over all contact pairs in the lattice. The addition of the new interactions would merely double the resulting value for the internal energy.

Resulting System of Equations

The system in equilibrium is calculated by minimizing the Helmholtz free energy. Inserting the just developed expressions for the internal energy and the entropy given at equations (4-30) and (4-29) into equation (3-7) yields the target function for the minimization.

$$\frac{A}{k_B N T} = \sum_{a,b,c,d} p_{a \cdot b \cdot c \cdot d} \left(\frac{\varepsilon_{ab}}{k_B T} + \frac{\varepsilon_{ac}}{k_B T} + \ln \left(\frac{p_{a \cdot b \cdot c \cdot d}}{\sum_a p_{a \cdot b \cdot c \cdot d}} \right) \right) \quad (4-31)$$

In addition to the free energy, constraints are necessary for this minimization. These consist of the approximation of the square cluster probabilities using conditional pair probabilities and the relationships between the pair probabilities.

$$p_{a \cdot b \cdot c \cdot d} = \frac{1}{2} \left(p_d p_{b|d} p_{c|d} \frac{p_a p_{b|a} p_{c|a}}{\sum_a p_a p_{b|a} p_{c|a}} + p_c p_{a|c} p_{d|c} \frac{p_b p_{a|b} p_{d|b}}{\sum_b p_b p_{a|b} p_{d|b}} \right) \quad (4-32)$$

The formula (4-32) describes 16 equations where the iterators a , b , c and d each take on the states 1 and 2. It is recommended that the number of variables is reduced by replacing three of the four conditional pair probabilities with their relationship to the fourth one.

$$\begin{aligned} p_{1|1} &= 1 - \frac{p_{1|2} p_2}{p_1} \\ p_{2|2} &= 1 - p_{1|2} \\ p_{2|1} &= \frac{p_{1|2} p_2}{p_1} \end{aligned} \quad (4-33)$$

The resulting system of equations consists of 20 equations and 21 variables which are the free energy A , the 4 conditional pair probabilities p_{ij} and the 16 cluster probabilities

$p_{a \cdot b \cdot c \cdot d}$. The equations (4-32) and (4-33) can be inserted into equation (4-31) which would yield one single equation dependent on one variable ($p_{1|2}$). This equation, however, can only be minimized numerically. Due to the size of the resulting equation it is in general recommended to work with the system of equations and constrained minimization instead.

4.2.1. Comparison to Guggenheim and Monte Carlo Simulations

Vinograd's second approximation is compared to Monte Carlo simulations, Guggenheim's quasi-chemical theory, and Vinograd's first approximation.

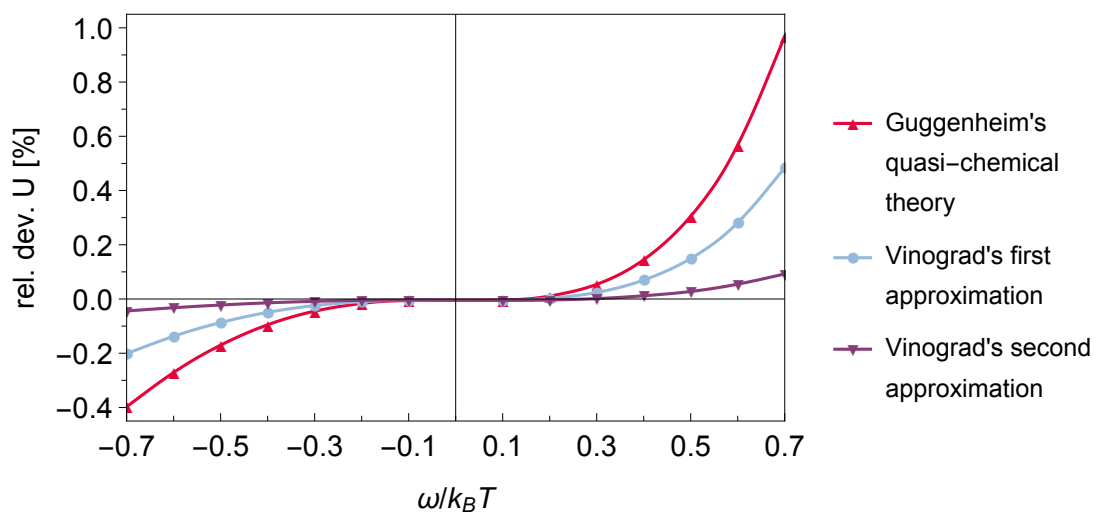


Figure 4-8.: Comparison of Vinograd's second approximation with MC-Simulations and Guggenheim: Internal Energy ($p_1 = 0.3$, $\varepsilon_{11} = \varepsilon_{22} = 0$, rel. dev. = $((\text{model} - \text{simulation}) / \text{simulation}) 100\%$)

The figures 4-8 and 4-9 show the relative deviation of the models with regard to the Monte Carlo simulation results. Figure 4-8 depicts the relative deviation of the internal energy and figure 4-9 shows the relative deviation of the entropy.

The second approximation is a significant improvement compared to the first approximation. The additional information of site B and C being connected with site D together with the symmetric lattice yields a much improved agreement with the Monte Carlo simulations.

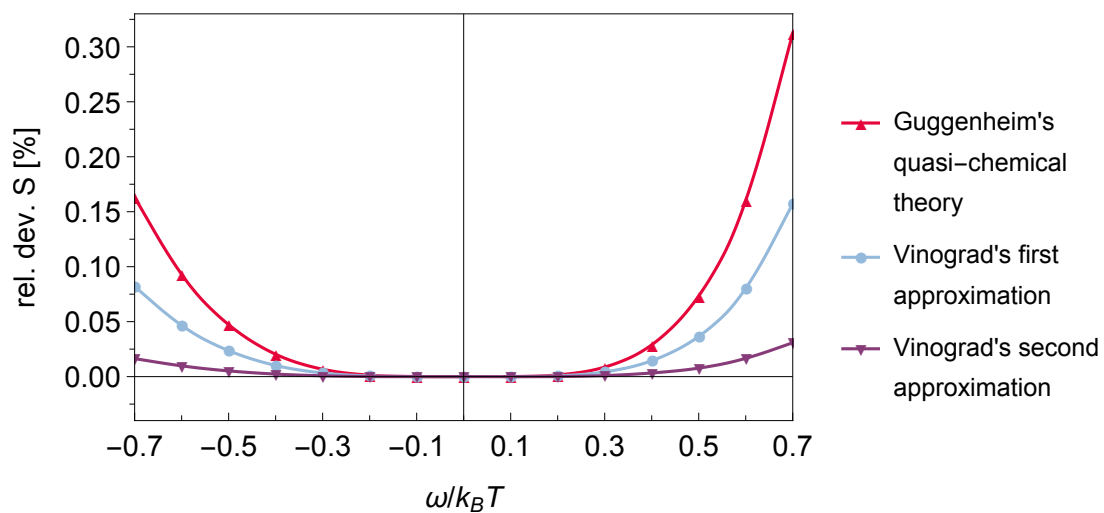


Figure 4-9.: Comparison of Vinograd's second approximation with MC-Simulations and Guggenheim: Entropy ($p_1 = 0.3, \varepsilon_{11} = \varepsilon_{22} = 0$, rel. dev. = $((\text{model} - \text{simulation}) / \text{simulation}) 100\%$)

4.2.2. Thermodynamic Consistency Check

The thermodynamic consistency check is performed according to the description in section 4.1.2.

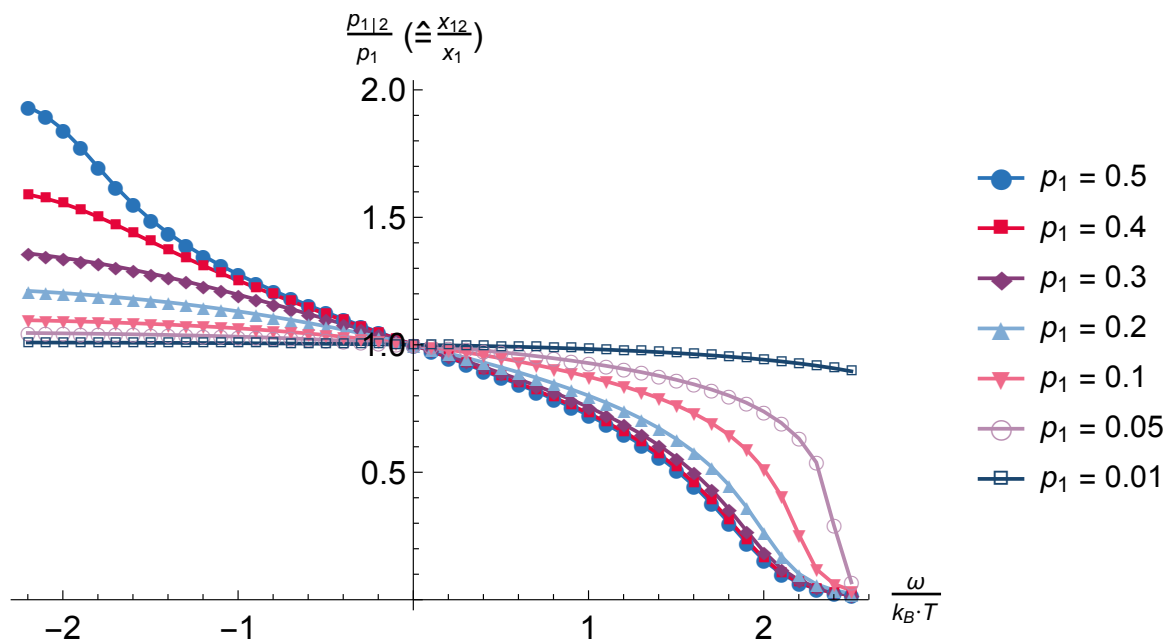


Figure 4-10.: 2D Vinograd's second approximation: $\frac{p_{1|2}}{p_1}$ over $\frac{\omega}{k_B T}$

Figure 4-10 shows this ratio of $p_{1|2}/p_1$ which can also be expressed as the ratio of the local composition to the global composition x_{12}/x_1 . The abscissa marks the dimensionless exchange energy $\omega/k_B T$ where the negative values denote an attraction

between the molecules of types 1 and 2 and the positive values denote a repulsion between the two. Each line in the figure represents one global composition.

Figure 4-10 illustrates that the second approximation converges significantly faster than the first approximation. This can be attributed to the consideration of more interactions between the molecules by including the site D .

4.3. Refinement of Vinograd's Second Approximation

A refined version of Vinograd's second approximation is developed. This modification has the intention of retaining the symmetric cluster probabilities, acquired in the second approximation while using the same entropy and energy formulas that the first approximation uses which are given by the equations (4-6) and (4-4). This can be achieved by taking the cluster probabilities from the second approximation, defined by equation (4-25), and applying the law of total probability. Therefore the probability

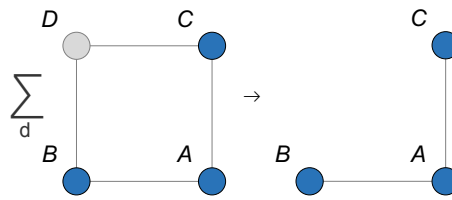


Figure 4-11.: Calculation of the a neighborhood from the square cluster

of the $a \cdot b \cdot c$ cluster is calculated via a summation of $p_{a \cdot b \cdot c \cdot d}$ over all possible states of d , as illustrated in figure 4-11.

$$p_{a \cdot b \cdot c} = \sum_d p_{a \cdot b \cdot c \cdot d} \quad (4-34)$$

Resulting System of Equations

The system in equilibrium is calculated by minimizing the Helmholtz free energy. The formula for the free energy of the refinement of Vinograd's second approximation expressed with cluster probabilities is the same as the one from Vinograd's first approximation which is given by equation (4-12).

$$\frac{A}{k_B N T} = \sum_{a,b,c} p_{a \cdot b \cdot c} \left(\frac{\varepsilon_{ab}}{k_B T} + \frac{\varepsilon_{ac}}{k_B T} + \ln \left(\frac{p_{a \cdot b \cdot c}}{\sum_a p_{a \cdot b \cdot c}} \right) \right) \quad (4-35)$$

The cluster probabilities expressed with conditional pair probabilities are the result of inserting equation (4-32), which describes the square cluster probabilities from the second approximation, into equation (4-34).

$$p_{a \cdot b \cdot c} = \frac{1}{2} \sum_d \left(p_d p_{b|d} p_{c|d} \frac{p_a p_{b|a} p_{c|a}}{\sum_a p_a p_{b|a} p_{c|a}} + p_c p_{a|c} p_{d|c} \frac{p_b p_{a|b} p_{d|b}}{\sum_b p_b p_{a|b} p_{d|b}} \right) \quad (4-36)$$

The formula (4-36) describes 8 equations where the iterators a , b , c and d each take on the states 1 and 2. Also, the correlations between the conditional pair probabilities

are needed. It is recommended to express three of the conditional pair probabilities as a function of the fourth, in order to reduce the number of variables.

$$\begin{aligned} p_{1|1} &= 1 - \frac{p_{1|2} p_2}{p_1} \\ p_{2|2} &= 1 - p_{1|2} \\ p_{2|1} &= \frac{p_{1|2} p_2}{p_1} \end{aligned} \quad (4-37)$$

The resulting system of equations consists of 12 equations and 13 variables which are the free energy A , the 4 conditional pair probabilities $p_{i|j}$ and the 8 cluster probabilities $p_{a \cdot b \cdot c}$. The equations (4-36) and (4-37) can be inserted into equation (4-35) which would yield one single equation dependent on one variable ($p_{1|2}$). This equation, however, can only be minimized numerically. Due to the size of the resulting equation it is in general recommended to work with the system of equations and constrained minimization instead.

4.3.1. Comparison to Guggenheim and Monte Carlo Simulations

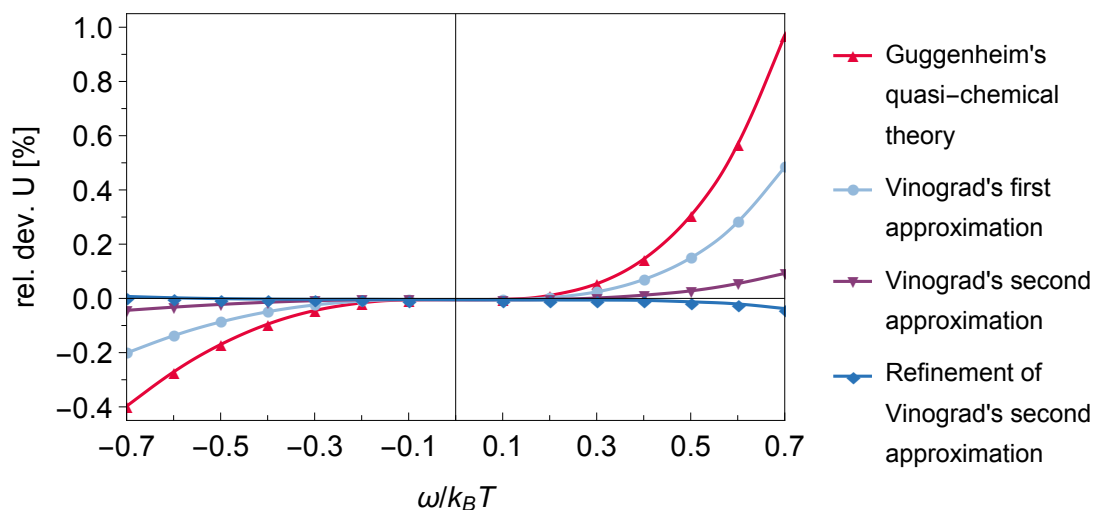


Figure 4-12.: Comparison of the refinement of Vinograd's second approximation with MC-Simulations and Guggenheim: Internal Energy ($p_1 = 0.3, \varepsilon_{11} = \varepsilon_{22} = 0$, rel. dev. = $((\text{model} - \text{simulation}) / \text{simulation}) 100\%$)

Figures 4-12 and 4-13 compare all two-dimensional models with each other regarding their relative deviations to Monte Carlo simulations. Figure 4-12 depicts the relative

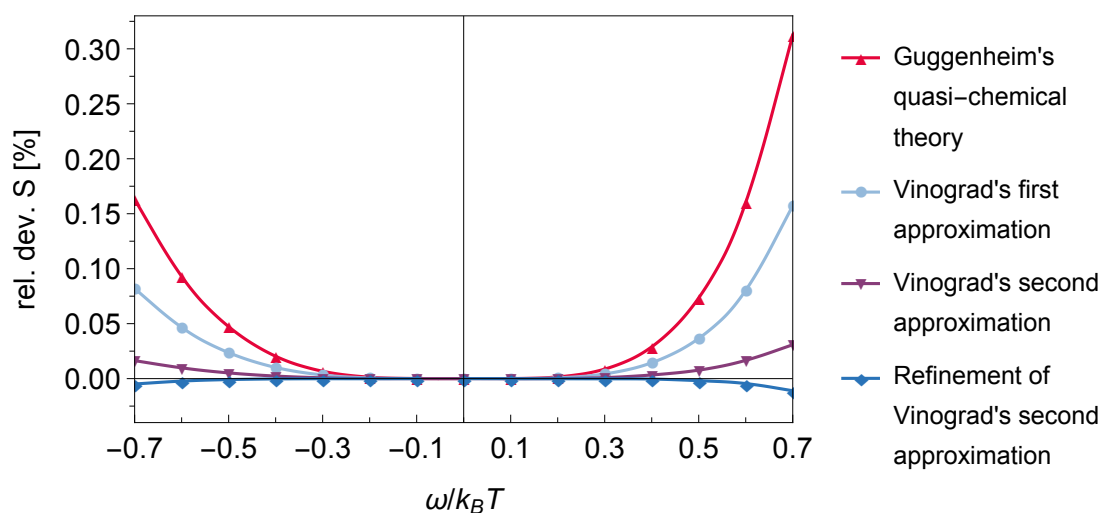


Figure 4-13.: Comparison of the refinement of Vinograd's second approximation with MC-Simulations and Guggenheim: Entropy ($p_1 = 0.3$, $\varepsilon_{11} = \varepsilon_{22} = 0$, rel. dev. = $((\text{model} - \text{simulation}) / \text{simulation}) 100\%$)

deviation of the internal energy and figure 4-13 shows the relative deviation of the entropy.

There are two main observations that can be gathered from the figures 4-12 and 4-13. The first property of the refinement of the second approximation that can be extracted from these figures is that the deviations are smaller than the ones from Vinograd's second approximation. A possible explanation for this might be that since we approximate the cluster by using pair probabilities the entropy formula containing just nearest neighbors is more appropriate. The consideration of the site D improves the neighborhood probabilities while the conditional probabilities retain the high accuracy that the first approximation shows.

The second is the fact that the relative deviations are negative. In all the previous models, however, the deviations are always positive. An explanation for this is, that the deviations of this model are so small that the inaccuracy of the Monte Carlo simulations is noticeable.

4.3.2. Thermodynamic Consistency Check

The thermodynamic consistency check is performed according to the description in section 4.1.2.

Figure 4-14 shows this ratio of p_{12}/p_1 which can also be expressed as the ratio of the local composition to the global composition x_{12}/x_1 . The abscissa marks the

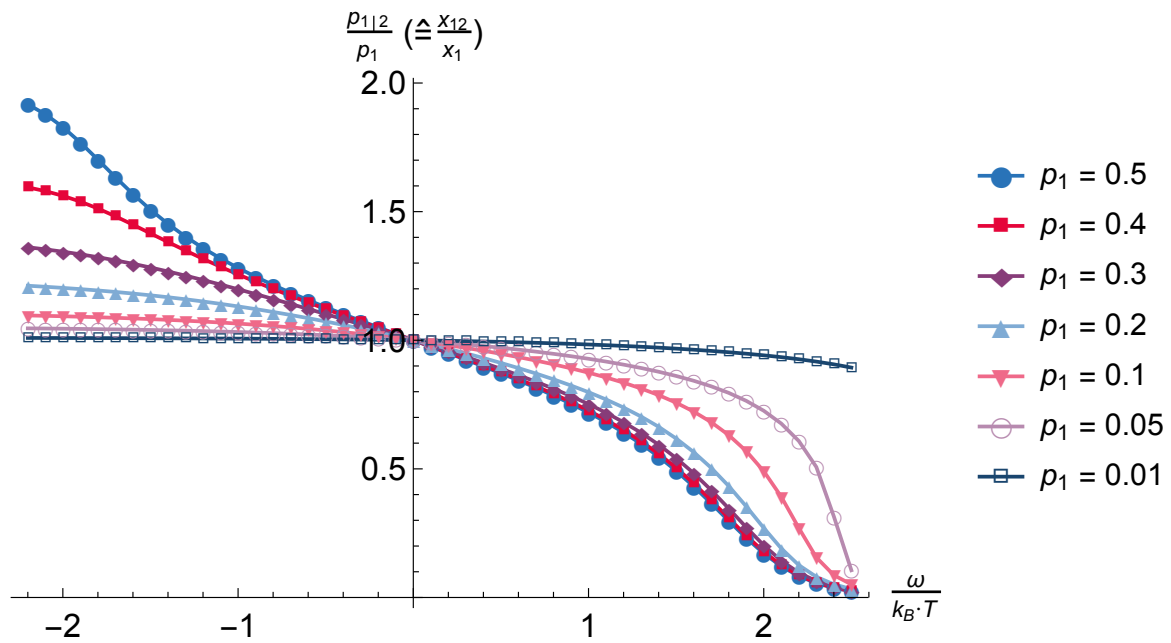


Figure 4-14.: 2D refinement of Vinograd's second approximation: $\frac{p_{1|2}}{p_1}$ over $\frac{\omega}{k_B T}$

dimensionless exchange energy $\omega/k_B T$ where the negative values denote an attraction between the molecules of types 1 and 2 and the positive values denote a repulsion between the two. Each line in the figure represents one global composition.

Figure 4-14 illustrates that the refinement of the second approximation behaves similarly to the second approximation. The similarity of the two models is expected, because no new interactions are considered.

4.4. Comparison of Models

This section provides a brief summary of the differences between the two-dimensional models. Guggenheim's quasi-chemical theory assumes that all pairs of contacts are independent from each other. This assumption leads to the fact that the quasi-chemical theory is the simplest model, but also the one with the largest deviations from the Monte Carlo simulations.

Vinograd's first approximation uses the sequential lattice construction to model the entropy. The pairs of contacts share the common site A but are still independent regarding all other sites. This results in a noticeable improvement over the quasi-chemical theory. Also, the first approximation yields an asymmetric lattice which means that not general relations between cluster probabilities are fulfilled.

Vinograd's second approximation solves the issue of the asymmetry by averaging all construction directions. A dependency of the neighbors of site A on site D is also introduced. The second approximation shows an improved agreement with the simulation data than the previous models.

The refinement of Vinograd's second approximation retains the beneficial properties of the second approximation and improves the modeling of the entropy. Therefore this model shows the smallest deviations from the Monte Carlo simulation data.

The next step is to apply the methods used to develop these models to a three-dimensional simple cubic lattice.

5. Simple Cubic Lattice (3D)

The three-dimensional cubic lattice is also constructed in a sequential manner. The lattice is built up layer by layer. Each new layer is constructed like the two-dimensional square lattice. The number of nearest neighbors that every new site is placed into increases to three.

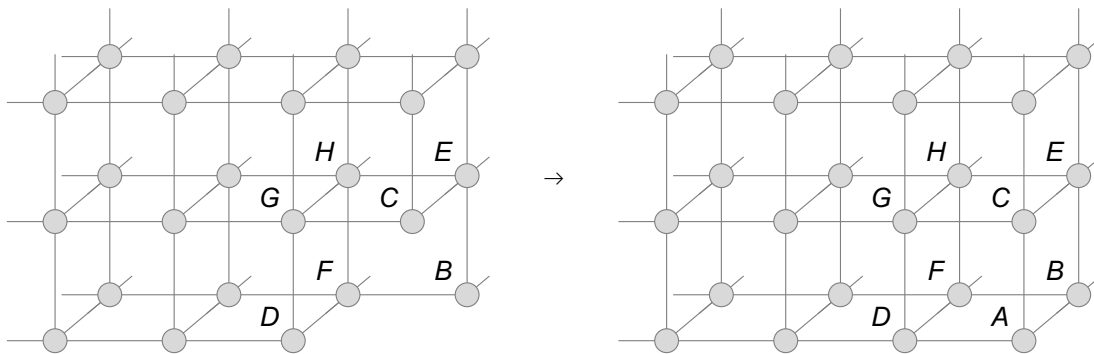


Figure 5-1.: 3D cubic lattice construction - addition of site A to the lattice

The figure 5-1 depicts the insertion of site A into the lattice. The three construction directions are from back to front, from top to bottom and from left to right. The addition of site A is dependent on its neighbors B, C and D. The sites B, C and D have no direct dependencies to one another. However, each pair of them has a common neighbor besides A. These neighbors are the sites E, F and G, which are all dependent on the site H.

The entropy can be formulated based on this lattice construction. It is the sum over all possible insertions a expressed as the insertion probability times its natural logarithm. All of these are weighted with each respective neighborhood probability and multiplied with minus the number of molecules in the system and Boltzmann's constant.

$$S = -Nk_B \sum_{b,c,d} p_{b \cdot c \cdot d} \sum_a p_{a|b \cdot c \cdot d} \ln(p_{a|b \cdot c \cdot d}) \quad (5-1)$$

By applying the definition of conditional probabilities to the probability of the insertion of molecule a , it can be expressed as the $a \cdot b \cdot c \cdot d$ cluster probability divided by the neighborhood probability.

$$p_{a|b \cdot c \cdot d} = \frac{p_{a \cdot b \cdot c \cdot d}}{p_{b \cdot c \cdot d}} \quad (5-2)$$

The neighborhood probabilities can be calculated from the cluster probabilities via a summation of all possible states of molecule a .

$$p_{b \cdot c \cdot d} = \sum_a p_{a \cdot b \cdot c \cdot d} \quad (5-3)$$

Equation (5-1) can be rewritten using cluster probabilities instead of conditional and neighborhood probabilities by inserting the equations (5-2) and (5-3).

$$S = -Nk_B \sum_{a,b,c,d} p_{a \cdot b \cdot c \cdot d} \ln \left(\frac{p_{a \cdot b \cdot c \cdot d}}{\sum_a p_{a \cdot b \cdot c \cdot d}} \right) \quad (5-4)$$

The internal energy is again modeled as the sum of all contact pairs weighted with each respective probability of occurrence.

$$U = N \sum_{b,c,d} p_{b \cdot c \cdot d} \sum_a p_{a|b \cdot c \cdot d} (\varepsilon_{ab} + \varepsilon_{ac} + \varepsilon_{ad}) \quad (5-5)$$

The internal energy can also be expressed in terms of cluster probabilities by applying equation (5-2) to equation (5-5).

$$U = N \sum_{a,b,c,d} p_{a \cdot b \cdot c \cdot d} (\varepsilon_{ab} + \varepsilon_{ac} + \varepsilon_{ad}) \quad (5-6)$$

All three-dimensional models are solved with a numerical minimization of the Helmholtz free energy under consideration of the dependencies between the pair probabilities given by equation (3-15). The Lagrange method for solving the system of equations has also been tested. The result of this investigation is the realization that no explicit solution for the models is possible. This method requires a higher computational effort than a minimization. Therefore, it is recommended that the equations are solved by applying a numerical minimization. Multiple models for approximating the cluster probabilities with pair probabilities are presented in the following sections.

5.1. Vinograd's First Approximation Applied to 3D

The first approximation, defined in section 4.1, is extended to be able to describe a three-dimensional lattice. The starting point of this model is equation (4-11) from the square lattice. This equation defines the cluster probability of a and its nearest neighbors as the probability of a times the probabilities of the neighbors depending on a . For the three-dimensional case, this can be expanded to include all three neighbors. The probability of the $a \cdot b \cdot c \cdot d$ cluster is thus approximated by the probability of a and the probabilities of b , c and d dependent on a .

$$p_{a \cdot b \cdot c \cdot d} = p_a p_{b|a} p_{c|a} p_{d|a} \quad (5-7)$$

Equation (5-7) represents the simplest possible approximation for the three-dimensional lattice. It has an asymmetry similar to the first approximation for the square lattice. The effect of this asymmetry is even more significant for the cubic lattice than for the square lattice.

Resulting System of Equations

The system in equilibrium is calculated by minimizing the Helmholtz free energy. Inserting the expressions for the internal energy and the entropy given at equations (5-6) and (5-4) into equation (3-7) yields the target function for the minimization.

$$\frac{A}{k_B N T} = \sum_{a,b,c,d} p_{a \cdot b \cdot c \cdot d} \left(\frac{\varepsilon_{ab}}{k_B T} + \frac{\varepsilon_{ac}}{k_B T} + \frac{\varepsilon_{ad}}{k_B T} + \ln \left(\frac{p_{a \cdot b \cdot c \cdot d}}{\sum_a p_{a \cdot b \cdot c \cdot d}} \right) \right) \quad (5-8)$$

The constraints of this optimization are the equations that connect the 16 cluster probabilities $p_{a \cdot b \cdot c \cdot d}$ to the four conditional pair probabilities $p_{a|b}$ given by formula (5-7).

$$p_{a \cdot b \cdot c \cdot d} = p_a p_{b|a} p_{c|a} p_{d|a} \quad (5-9)$$

The formula (5-9) describes 16 equations where the iterators a , b , c and d each take on the states 1 and 2. Also, the correlations between the conditional pair probabilities are needed. It is recommended to express three of the conditional pair probabilities

as a function of the fourth, in order to reduce the number of variables. The formulas that are given by equation (3-15) are therefore transformed into the following form.

$$\begin{aligned} \rho_{1|1} &= 1 - \frac{\rho_{1|2} \rho_2}{\rho_1} \\ \rho_{2|2} &= 1 - \rho_{1|2} \\ \rho_{2|1} &= \frac{\rho_{1|2} \rho_2}{\rho_1} \end{aligned} \quad (5-10)$$

The resulting system of equations consists of 20 equations and 21 variables which are the free energy A , the 4 conditional pair probabilities ρ_{ij} and the 16 cluster probabilities $\rho_{a \cdot b \cdot c \cdot d}$. The equations (5-9) and (5-10) can be inserted into equation (5-8) which would yield one single equation dependent on one variable ($\rho_{1|2}$). This equation, however, can only be minimized numerically. Due to the size of the resulting equation it is in general recommended to work with the system of equations and constrained minimization instead.

5.1.1. Comparison to Guggenheim and Monte Carlo Simulations

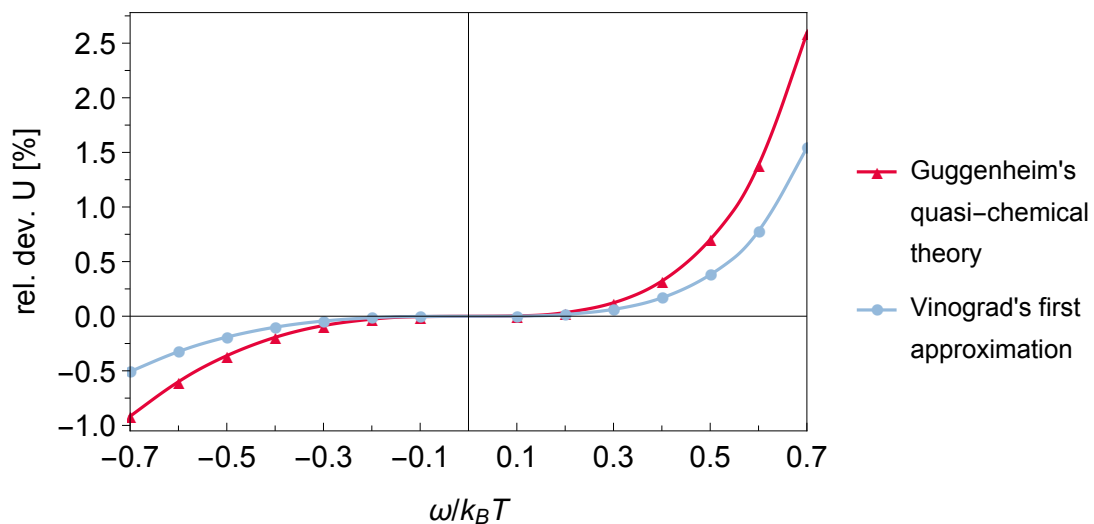


Figure 5-2.: Comparison of 3D Vinograd's first approximation with MC-Simulations and Guggenheim: Internal Energy ($\rho_1 = 0.3, \varepsilon_{11} = \varepsilon_{22} = 0$, rel. dev. = $((\text{model} - \text{simulation}) / \text{simulation}) 100\%$)

Vinograd's first approximation applied to 3D is compared to Monte Carlo simulation results in order to assess the quality of this model. Guggenheim's quasi-chemical approach is used as a reference model.

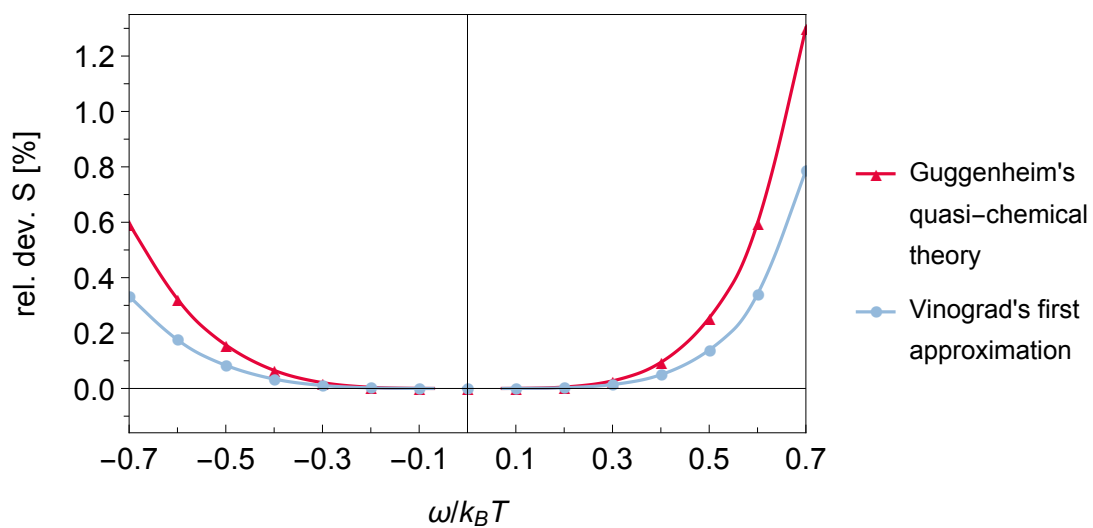


Figure 5-3.: Comparison of 3D Vinograd's first approximation with MC-Simulations and Guggenheim: Entropy ($p_1 = 0.3, \varepsilon_{11} = \varepsilon_{22} = 0$, rel. dev. = $((\text{model} - \text{simulation}) / \text{simulation}) 100\%$)

The figures 5-2 and 5-3 show the relative deviation of Vinograd's first approximation applied to 3D and Guggenheim's quasi-chemical theory to the Monte Carlo simulation results. Figure 5-2 depicts the relative deviation of the internal energy and figure 5-3 shows the relative deviation of the entropy.

The figures 5-2 and 5-3 indicate that the assumptions made for this model are not that dissimilar to the assumptions of the quasi-chemical theory. The deviations of this model from the Monte Carlo simulations show only a slight improvement over the quasi-chemical theory.

5.1.2. Thermodynamic Consistency Check

The thermodynamic consistency check is performed according to the description in section 4.1.2.

Figure 5-4 shows this ratio of $p_{1|2}/p_1$ which can also be expressed as the ratio of the local composition to the global composition x_{12}/x_1 . The abscissa marks the dimensionless exchange energy $\omega/k_B T$ where the negative values denote an attraction between the molecules of types 1 and 2 and the positive values denote a repulsion between the two. Each line in the figure represents one global composition.

Figure 5-4 indicates that even though the model approaches the limits, it does so quite slowly. This slow convergence is caused by the assumption of independence of the pairs of molecules, which is the basis of Vinograd's first approximation. However, the

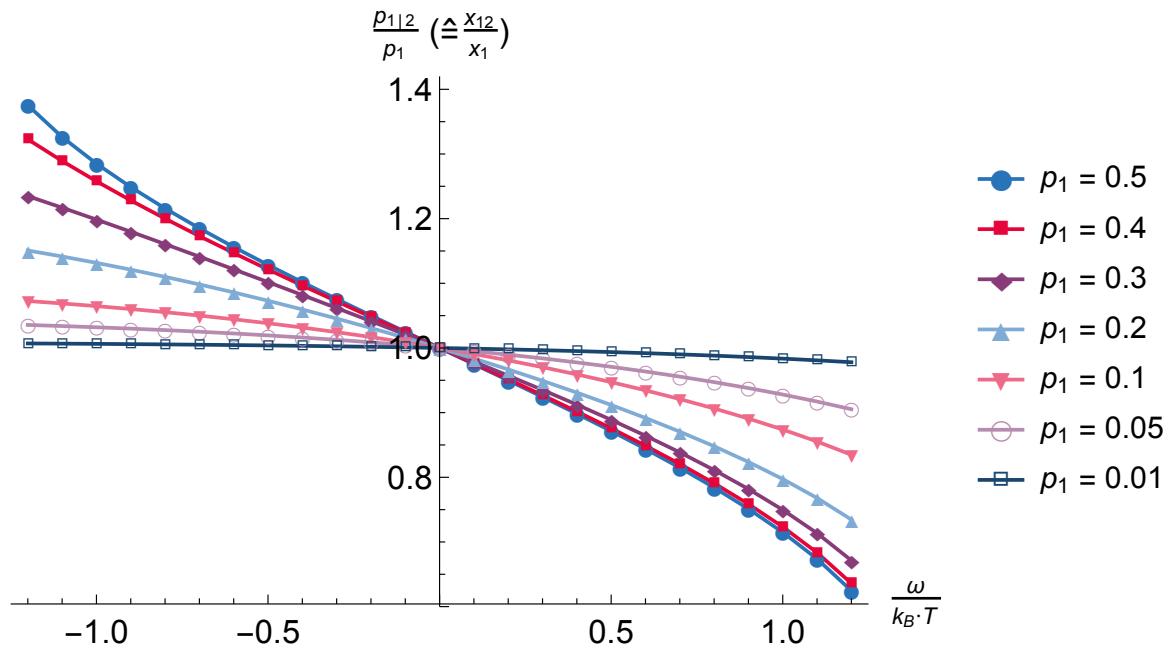


Figure 5-4.: 3D Vinograd's first approximation: $\frac{p_{1|2}}{p_1}$ over $\frac{\omega}{k_B T}$

three-dimensional model converges quicker than the two-dimensional one. This can be explained with the fact that the three-dimensional lattice contains more interactions of the molecules than the two-dimensional lattice.

5.2. Vinograd's Second Approximation Applied to 3D

An eight site cluster containing sites A to H is considered for Vinograd's second approximation applied to 3D. As with the square cluster, this cubic cluster is approximated by using pair probabilities. Special attention has to be given to the averaging of all construction directions.

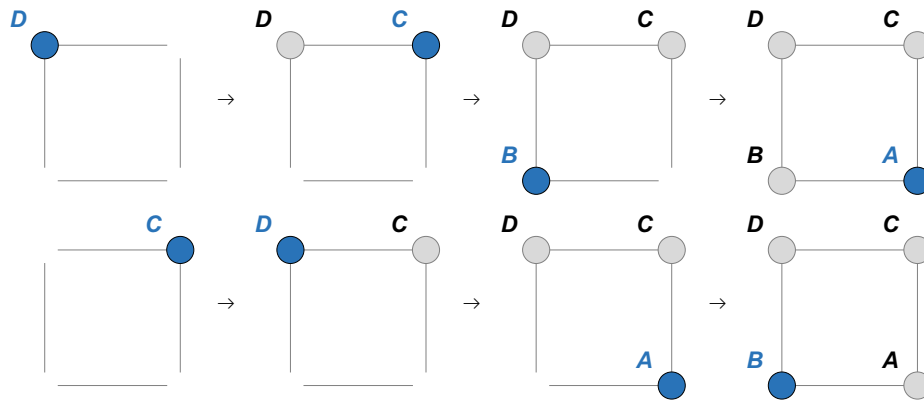


Figure 5-5.: Square cluster construction directions

Figure 5-5 displays the two construction directions that need to be considered in order to create a symmetric square cluster. The resulting formula is developed in equations (4-21) to (4-25).

$$p_{a \cdot b \cdot c \cdot d}^{sq} = \frac{1}{2} (p_d p_{c|d} p_{b|d} p_{a|b \cdot c} + p_c p_{d|c} p_{a|c} p_{b|a \cdot d}) \quad (5-11)$$

It is possible to use these symmetric probabilities of the square cluster for the construction of the cubic cluster. The sq at the cluster probability denotes the fact that this is the probability of the square cluster and exists to avoid confusion with the three-dimensional four site cluster formed by A and its nearest neighbors. The conditional probability of the addition of two neighboring sites depending on the two other sites can be calculated by applying the law of total probability to this cluster.

$$p_{a \cdot b|d \cdot f} = \frac{p_{a \cdot b \cdot d \cdot f}^{sq}}{p_{d \cdot f}} = \frac{p_{a \cdot b \cdot d \cdot f}^{sq}}{\sum_{a,b} p_{a \cdot b \cdot d \cdot f}^{sq}} \quad (5-12)$$

Figure 5-6 shows one construction direction of the cubic cluster. The starting point is the $a \cdot b \cdot d \cdot f$ cluster. Next, the $c \cdot e$ cluster is inserted with dependencies to a and b .

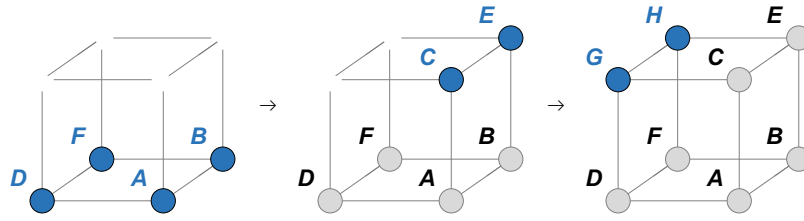


Figure 5-6.: Cubic cluster construction from square cluster

This newly formed L -shaped cluster can be used to calculate the probability of $g \cdot h$ depending on c, d, e and f .

$$p_{a \cdot b | c \cdot e \cdot d \cdot f} = \frac{p_{a \cdot b \cdot d \cdot f}^{sq} p_{c \cdot e | a \cdot b}}{\sum_{a,b} p_{a \cdot b \cdot d \cdot f}^{sq} p_{c \cdot e | a \cdot b}} \quad (5-13)$$

This procedure has to be averaged over the different construction directions.

Again, because of the structure of the equations, not all construction directions have to be considered. Figure 5-7 shows the six construction directions which suffice to generate a symmetric cluster.

$$p_{a \cdot b \cdot c \cdot d \cdot e \cdot f \cdot g \cdot h} = \frac{1}{6} (p_{a \cdot b \cdot d \cdot f}^{sq} p_{c \cdot e | a \cdot b} p_{g \cdot h | c \cdot e \cdot d \cdot f} + p_{a \cdot c \cdot b \cdot e}^{sq} p_{d \cdot g | a \cdot c} p_{f \cdot h | d \cdot g \cdot b \cdot e} + p_{a \cdot d \cdot b \cdot f}^{sq} p_{c \cdot g | a \cdot d} p_{e \cdot h | b \cdot f \cdot c \cdot g} + p_{c \cdot e \cdot a \cdot b}^{sq} p_{g \cdot h | c \cdot e} p_{d \cdot f | g \cdot h \cdot a \cdot b} + p_{b \cdot e \cdot a \cdot c}^{sq} p_{f \cdot h | b \cdot e} p_{d \cdot g | f \cdot h \cdot a \cdot c} + p_{c \cdot g \cdot a \cdot d}^{sq} p_{e \cdot h | c \cdot g} p_{b \cdot f | e \cdot h \cdot a \cdot d}) \quad (5-14)$$

One might think that as an alternative it would be possible to construct the cubic cluster similar to the square cluster by starting in one corner, sequentially add sites till the opposite corner is reached and averaging the eight construction directions starting at each corner. This method would, however, still return an asymmetric cluster. Therefore the previously described procedure is necessary.

The equation for the entropy of the lattice is formulated using the probability of the insertion of a into the b, c, d, e, f, g and h neighborhood.

$$S = -k_B N \sum_{b,c,d,e,f,g,h} p_{b \cdot c \cdot d \cdot e \cdot f \cdot g \cdot h} \sum_a p_{a | b \cdot c \cdot d \cdot e \cdot f \cdot g \cdot h} \ln (p_{a | b \cdot c \cdot d \cdot e \cdot f \cdot g \cdot h}) \quad (5-15)$$

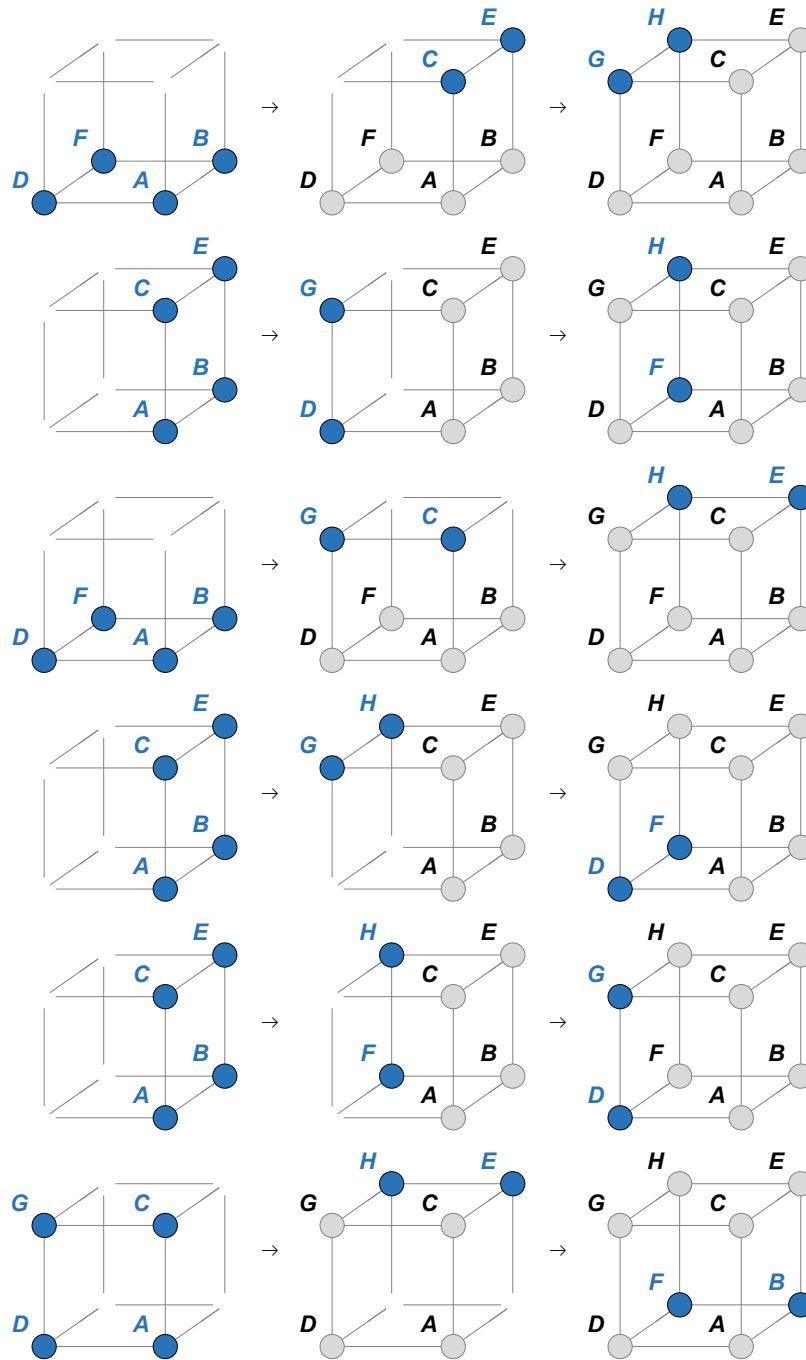


Figure 5-7.: Cubic cluster construction directions

The probability of the insertion of molecule a can be expressed as the ratio of the cluster probability to the neighborhood probability.

$$p_{a|b \cdot c \cdot d \cdot e \cdot f \cdot g \cdot h} = \frac{p_{a \cdot b \cdot c \cdot d \cdot e \cdot f \cdot g \cdot h}}{p_{b \cdot c \cdot d \cdot e \cdot f \cdot g \cdot h}} \quad (5-16)$$

The neighborhood probability can be expressed as the summation of the cluster probabilities over all possibilities of a .

$$p_{b \cdot c \cdot d \cdot e \cdot f \cdot g \cdot h} = \sum_a p_{a \cdot b \cdot c \cdot d \cdot e \cdot f \cdot g \cdot h} \quad (5-17)$$

Rewritten in terms of cluster probabilities, by combining equations (5-15), (5-16) and (5-17), the equation for the entropy yields:

$$S = -k_B N \sum_{a,b,c,d,e,f,g,h} p_{a \cdot b \cdot c \cdot d \cdot e \cdot f \cdot g \cdot h} \ln \left(\frac{p_{a \cdot b \cdot c \cdot d \cdot e \cdot f \cdot g \cdot h}}{\sum_a p_{a \cdot b \cdot c \cdot d \cdot e \cdot f \cdot g \cdot h}} \right) \quad (5-18)$$

The internal energy of this model is calculated as a weighted sum of the interaction energies of all pairs. The three new pairs that are formed during the insertion of molecule a describe all pairs of molecules in the lattice.

$$U = N \sum_{b,c,d,e,f,g,h} p_{b \cdot c \cdot d \cdot e \cdot f \cdot g \cdot h} \sum_a p_{a|b \cdot c \cdot d \cdot e \cdot f \cdot g \cdot h} (\varepsilon_{ab} + \varepsilon_{ac} + \varepsilon_{ad}) \quad (5-19)$$

The equation for the internal energy can be expressed using cluster probabilities by combining equations (5-16) and (5-19).

$$U = N \sum_{a,b,c,d,e,f,g,h} p_{a \cdot b \cdot c \cdot d \cdot e \cdot f \cdot g \cdot h} (\varepsilon_{ab} + \varepsilon_{ac} + \varepsilon_{ad}) \quad (5-20)$$

Resulting System of Equations

The system in equilibrium is calculated by minimizing the Helmholtz free energy. Inserting the expressions for the internal energy and the entropy given at equations (5-18) and (5-20) into equation (3-7) yields the target function for the minimization.

$$\frac{A}{k_B N T} = \sum_{a,b,c,d,e,f,g,h} p_{a \cdot b \cdot c \cdot d \cdot e \cdot f \cdot g \cdot h} \left(\frac{\varepsilon_{ab}}{k_B T} + \frac{\varepsilon_{ac}}{k_B T} + \frac{\varepsilon_{ad}}{k_B T} + \ln \left(\frac{p_{a \cdot b \cdot c \cdot d \cdot e \cdot f \cdot g \cdot h}}{\sum_a p_{a \cdot b \cdot c \cdot d \cdot e \cdot f \cdot g \cdot h}} \right) \right) \quad (5-21)$$

The constraints of this optimization are the equations that connect the 256 cluster probabilities $p_{a \cdot b \cdot c \cdot d \cdot e \cdot f \cdot g \cdot h}$ to the four conditional pair probabilities $p_{a|b}$.

$$\begin{aligned}
 p_{a \cdot b \cdot c \cdot d \cdot e \cdot f \cdot g \cdot h} = \frac{1}{6} & \left(\frac{p_{a \cdot d \cdot b \cdot f}^{sq} p_{c \cdot g \cdot a \cdot d}^{sq} p_{b \cdot f \cdot e \cdot h}^{sq} p_{e \cdot h \cdot c \cdot g}^{sq}}{\left(\sum_{c,g} p_{c \cdot g \cdot a \cdot d}^{sq} \right) \left(\sum_{b,f} p_{b \cdot f \cdot e \cdot h}^{sq} \right) \sum_{e,h} \frac{p_{b \cdot f \cdot e \cdot h}^{sq} p_{e \cdot h \cdot c \cdot g}^{sq}}{\sum_{b,f} p_{b \cdot f \cdot e \cdot h}^{sq}}} \right. \\
 & + \frac{p_{b \cdot f \cdot a \cdot d}^{sq} p_{c \cdot g \cdot a \cdot d}^{sq} p_{e \cdot h \cdot b \cdot f}^{sq} p_{e \cdot h \cdot c \cdot g}^{sq}}{\left(\sum_{e,h} p_{e \cdot h \cdot b \cdot f}^{sq} \right) \left(\sum_{e,h} p_{e \cdot h \cdot c \cdot g}^{sq} \right) \sum_{b,f} \frac{p_{b \cdot f \cdot a \cdot d}^{sq} p_{e \cdot h \cdot b \cdot f}^{sq}}{\sum_{e,h} p_{e \cdot h \cdot b \cdot f}^{sq}}} \\
 & + \frac{p_{c \cdot e \cdot a \cdot b}^{sq} p_{a \cdot b \cdot d \cdot f}^{sq} p_{c \cdot e \cdot g \cdot h}^{sq} p_{g \cdot h \cdot d \cdot f}^{sq}}{\left(\sum_{c,e} p_{c \cdot e \cdot a \cdot b}^{sq} \right) \left(\sum_{c,e} p_{c \cdot e \cdot g \cdot h}^{sq} \right) \sum_{g,h} \frac{p_{c \cdot e \cdot g \cdot h}^{sq} p_{g \cdot h \cdot d \cdot f}^{sq}}{\sum_{c,e} p_{c \cdot e \cdot g \cdot h}^{sq}}} \\
 & + \frac{p_{a \cdot c \cdot b \cdot e}^{sq} p_{d \cdot g \cdot a \cdot c}^{sq} p_{f \cdot h \cdot b \cdot e}^{sq} p_{d \cdot g \cdot f \cdot h}^{sq}}{\left(\sum_{d,g} p_{d \cdot g \cdot a \cdot c}^{sq} \right) \left(\sum_{d,g} p_{d \cdot g \cdot f \cdot h}^{sq} \right) \sum_{f,h} \frac{p_{f \cdot h \cdot b \cdot e}^{sq} p_{d \cdot g \cdot f \cdot h}^{sq}}{\sum_{d,g} p_{d \cdot g \cdot f \cdot h}^{sq}}} \\
 & + \frac{p_{b \cdot e \cdot a \cdot c}^{sq} p_{d \cdot g \cdot a \cdot c}^{sq} p_{f \cdot h \cdot b \cdot e}^{sq} p_{f \cdot h \cdot d \cdot g}^{sq}}{\left(\sum_{f,h} p_{f \cdot h \cdot b \cdot e}^{sq} \right) \left(\sum_{f,h} p_{f \cdot h \cdot d \cdot g}^{sq} \right) \sum_{d,g} \frac{p_{d \cdot g \cdot a \cdot c}^{sq} p_{f \cdot h \cdot d \cdot g}^{sq}}{\sum_{f,h} p_{f \cdot h \cdot d \cdot g}^{sq}}} \\
 & \left. + \frac{p_{c \cdot e \cdot a \cdot b}^{sq} p_{d \cdot f \cdot a \cdot b}^{sq} p_{g \cdot h \cdot c \cdot e}^{sq} p_{g \cdot h \cdot d \cdot f}^{sq}}{\left(\sum_{g,h} p_{g \cdot h \cdot c \cdot e}^{sq} \right) \left(\sum_{g,h} p_{g \cdot h \cdot d \cdot f}^{sq} \right) \sum_{d,f} \frac{p_{d \cdot f \cdot a \cdot b}^{sq} p_{g \cdot h \cdot d \cdot f}^{sq}}{\sum_{g,h} p_{g \cdot h \cdot d \cdot f}^{sq}}} \right) \quad (5-22)
 \end{aligned}$$

The formula (5-22) describes 256 equations where the iterators a, b, c, d, e, f, g and h each take on the states 1 and 2. The cubic cluster probabilities are expressed in terms of the square cluster probabilities. In addition to that, equation (5-11) after insertion of equation (4-24) is used which connects the 16 square cluster probabilities to the pair probabilities.

$$p_{a \cdot b \cdot c \cdot d}^{sq} = \frac{1}{2} \left(p_d p_{b|d} p_{c|d} \frac{p_a p_{b|a} p_{c|a}}{\sum_a p_a p_{b|a} p_{c|a}} + p_c p_{a|c} p_{d|c} \frac{p_b p_{a|b} p_{d|b}}{\sum_b p_b p_{a|b} p_{d|b}} \right) \quad (5-23)$$

Also, the correlations between the conditional pair probabilities are needed. It is recommended to express three of the conditional pair probabilities as a function of

the fourth, in order to reduce the number of variables. The formulas that are given by equation (3-15) are therefore transformed into the following form.

$$\begin{aligned} p_{1|1} &= 1 - \frac{p_{1|2} p_2}{p_1} \\ p_{2|2} &= 1 - p_{1|2} \\ p_{2|1} &= \frac{p_{1|2} p_2}{p_1} \end{aligned} \quad (5-24)$$

The resulting system of equations consists of 276 equations and 277 variables which are the free energy A , the 4 conditional pair probabilities p_{ij} , the 16 square cluster probabilities $p_{a \cdot b \cdot c \cdot d}^{sq}$ and the 256 cluster probabilities $p_{a \cdot b \cdot c \cdot d \cdot e \cdot f \cdot g \cdot h}$. The equations (5-22), (5-23) and (5-24) can be inserted into equation (5-21) which would yield one single equation dependent on one variable ($p_{1|2}$). This equation, however, can only be minimized numerically. Due to the size of the resulting equation it is in general recommended to work with the system of equations and constrained minimization instead.

5.2.1. Comparison to Guggenheim and Monte Carlo Simulations

Vinograd's second approximation applied to 3D is compared to Monte Carlo simulation results in order to assess the quality of this model. Guggenheim's quasi-chemical approach and the first approximation are used as reference models.

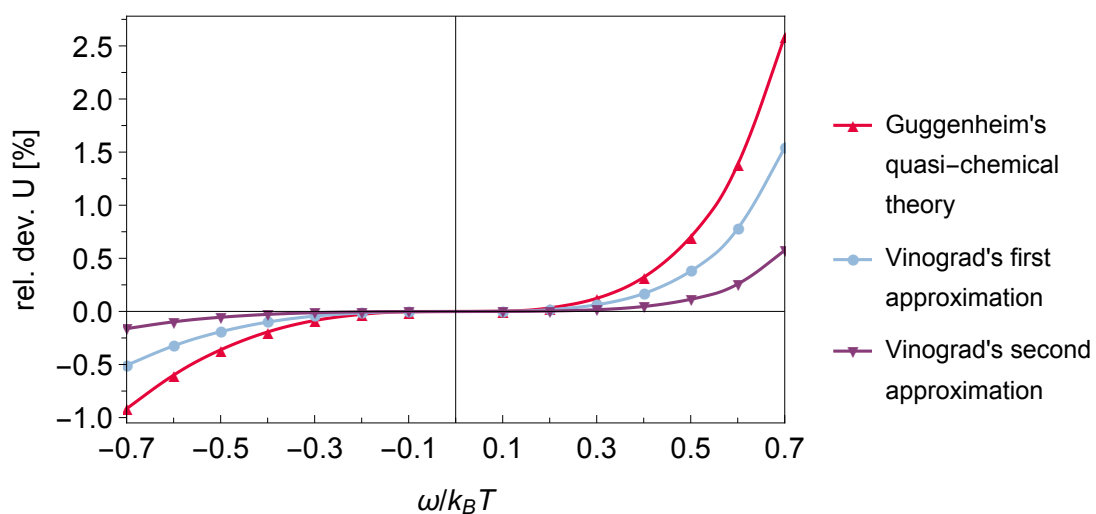


Figure 5-8.: Comparison of 3D Vinograd's second approximation with MC-Simulations and Guggenheim: Internal Energy ($p_1 = 0.3$, $\varepsilon_{11} = \varepsilon_{22} = 0$, rel. dev. = $((\text{model} - \text{simulation}) / \text{simulation}) 100\%$)

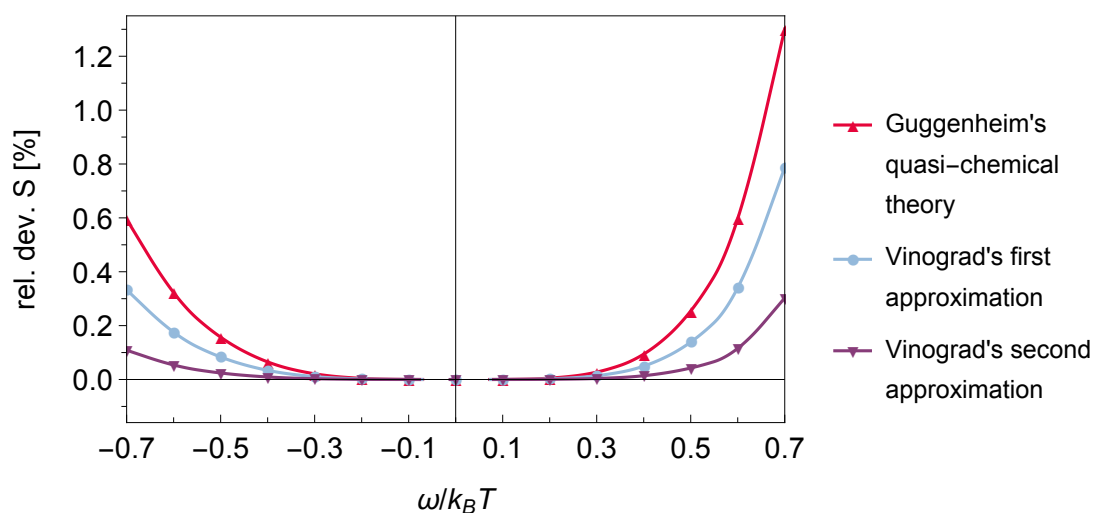


Figure 5-9.: Comparison of 3D Vinograd's second approximation with MC-Simulations and Guggenheim: Entropy ($p_1 = 0.3, \varepsilon_{11} = \varepsilon_{22} = 0$, rel. dev. = $((\text{model} - \text{simulation}) / \text{simulation}) 100\%$)

The figures 5-8 and 5-9 show the relative deviation of Vinograd's second approximation applied to 3D, Vinograd's first approximation applied to 3D and Guggenheim's quasi-chemical theory to the Monte Carlo simulation results. Figure 5-8 depicts the relative deviation of the internal energy and figure 5-9 shows the relative deviation of the entropy.

The figures 5-8 and 5-9 indicate that the second approximation applied to 3D has significant smaller deviations than the quasi-chemical theory and the first approximation.

5.2.2. Thermodynamic Consistency Check

The thermodynamic consistency check is performed according to the description in section 4.1.2.

Figure 5-10 illustrates this ratio of $p_{1|2}/p_1$ which can also be expressed as the ratio of the local composition to the global composition x_{12}/x_1 . The abscissa marks the dimensionless exchange energy $\omega/k_B T$ where the negative values denote an attraction between the molecules of types 1 and 2 and the positive values denote a repulsion between the two. Each line in the figure represents one global composition.

Figure 5-10 shows that the three-dimensional second approximation converges significantly faster than the first approximation. This can be attributed to the consideration of more interactions between the molecules and the symmetric cluster probabilities.

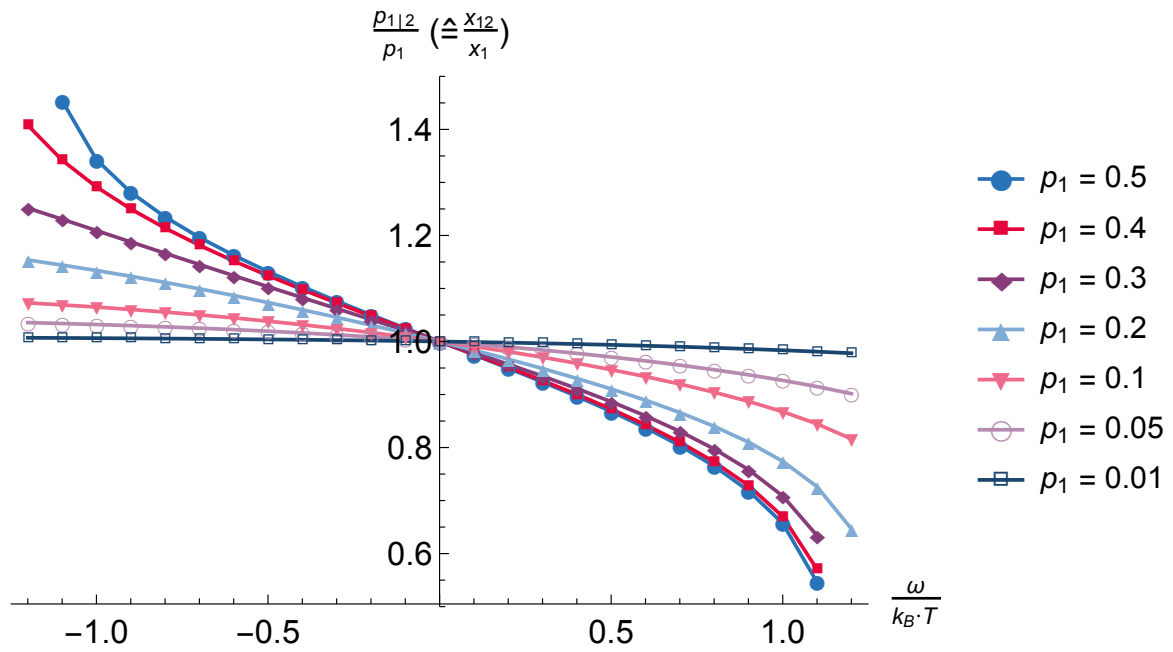


Figure 5-10.: 3D Vinograd's second approximation: $\frac{\rho_{1|2}}{\rho_1}$ over $\frac{\omega}{k_B T}$

5.3. Refinement of Vinograd's Second Approximation

The basis of the refinement of the second approximation is the eight site cubic cluster introduced in the second approximation (section 5.2). This cluster is used to improve the description of the neighborhood that the new molecule is placed into. The entropy and internal energy are modeled based on the insertion of a into its direct neighborhood. Their definitions are given in equations (5-4) and (5-6).

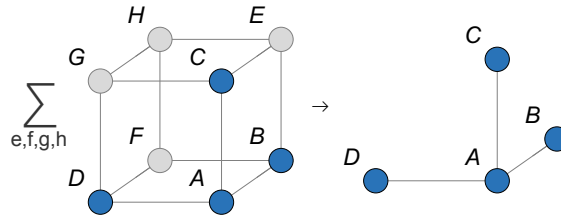


Figure 5-11.: Calculation of the a neighborhood from the cubic cluster

The conversion of the cubic cluster to the smaller cluster is achieved by applying the law of total probability. The sum of the probabilities of all possible states of e , f , g and h is formed, as illustrated in figure 5-11.

$$\rho_{a \cdot b \cdot c \cdot d} = \sum_{e, f, g, h} \rho_{a \cdot b \cdot c \cdot d \cdot e \cdot f \cdot g \cdot h} \quad (5-25)$$

Resulting System of Equations

The system in equilibrium is calculated by minimizing the Helmholtz free energy. Inserting the expressions for the internal energy and the entropy given at equations (5-6) and (5-4) into equation (3-7) yields the target function for the minimization.

$$\frac{A}{k_B N T} = \sum_{a, b, c, d} \rho_{a \cdot b \cdot c \cdot d} \left(\frac{\varepsilon_{ab}}{k_B T} + \frac{\varepsilon_{ac}}{k_B T} + \frac{\varepsilon_{ad}}{k_B T} + \ln \left(\frac{\rho_{a \cdot b \cdot c \cdot d}}{\sum_a \rho_{a \cdot b \cdot c \cdot d}} \right) \right) \quad (5-26)$$

The constraints of this optimization are the equations that connect the 16 cluster probabilities $p_{a \cdot b \cdot c \cdot d}$ to the four conditional pair probabilities $p_{a|b}$.

$$\begin{aligned}
 p_{a \cdot b \cdot c \cdot d} = \frac{1}{6} \sum_{e,f,g,h} \left(\right. & \frac{p_{a \cdot d \cdot b \cdot f}^{sq} p_{c \cdot g \cdot a \cdot d}^{sq} p_{b \cdot f \cdot e \cdot h}^{sq} p_{e \cdot h \cdot c \cdot g}^{sq}}{\left(\sum_{c,g} p_{c \cdot g \cdot a \cdot d}^{sq} \right) \left(\sum_{b,f} p_{b \cdot f \cdot e \cdot h}^{sq} \right) \sum_{e,h} \frac{p_{b \cdot f \cdot e \cdot h}^{sq} p_{e \cdot h \cdot c \cdot g}^{sq}}{\sum_{b,f} p_{b \cdot f \cdot e \cdot h}^{sq}}} \\
 & + \frac{p_{b \cdot f \cdot a \cdot d}^{sq} p_{c \cdot g \cdot a \cdot d}^{sq} p_{e \cdot h \cdot b \cdot f}^{sq} p_{e \cdot h \cdot c \cdot g}^{sq}}{\left(\sum_{e,h} p_{e \cdot h \cdot b \cdot f}^{sq} \right) \left(\sum_{e,h} p_{e \cdot h \cdot c \cdot g}^{sq} \right) \sum_{b,f} \frac{p_{b \cdot f \cdot a \cdot d}^{sq} p_{e \cdot h \cdot b \cdot f}^{sq}}{\sum_{e,h} p_{e \cdot h \cdot b \cdot f}^{sq}}} \\
 & + \frac{p_{c \cdot e \cdot a \cdot b}^{sq} p_{a \cdot b \cdot d \cdot f}^{sq} p_{c \cdot e \cdot g \cdot h}^{sq} p_{g \cdot h \cdot d \cdot f}^{sq}}{\left(\sum_{c,e} p_{c \cdot e \cdot a \cdot b}^{sq} \right) \left(\sum_{c,e} p_{c \cdot e \cdot g \cdot h}^{sq} \right) \sum_{g,h} \frac{p_{c \cdot e \cdot g \cdot h}^{sq} p_{g \cdot h \cdot d \cdot f}^{sq}}{\sum_{c,e} p_{c \cdot e \cdot g \cdot h}^{sq}}} \\
 & + \frac{p_{a \cdot c \cdot b \cdot e}^{sq} p_{d \cdot g \cdot a \cdot c}^{sq} p_{f \cdot h \cdot b \cdot e}^{sq} p_{d \cdot g \cdot f \cdot h}^{sq}}{\left(\sum_{d,g} p_{d \cdot g \cdot a \cdot c}^{sq} \right) \left(\sum_{d,g} p_{d \cdot g \cdot f \cdot h}^{sq} \right) \sum_{f,h} \frac{p_{f \cdot h \cdot b \cdot e}^{sq} p_{d \cdot g \cdot f \cdot h}^{sq}}{\sum_{d,g} p_{d \cdot g \cdot f \cdot h}^{sq}}} \\
 & + \frac{p_{b \cdot e \cdot a \cdot c}^{sq} p_{d \cdot g \cdot a \cdot c}^{sq} p_{f \cdot h \cdot b \cdot e}^{sq} p_{f \cdot h \cdot d \cdot g}^{sq}}{\left(\sum_{f,h} p_{f \cdot h \cdot b \cdot e}^{sq} \right) \left(\sum_{f,h} p_{f \cdot h \cdot d \cdot g}^{sq} \right) \sum_{d,g} \frac{p_{d \cdot g \cdot a \cdot c}^{sq} p_{f \cdot h \cdot d \cdot g}^{sq}}{\sum_{f,h} p_{f \cdot h \cdot d \cdot g}^{sq}}} \\
 & \left. + \frac{p_{c \cdot e \cdot a \cdot b}^{sq} p_{d \cdot f \cdot a \cdot b}^{sq} p_{g \cdot h \cdot c \cdot e}^{sq} p_{g \cdot h \cdot d \cdot f}^{sq}}{\left(\sum_{g,h} p_{g \cdot h \cdot c \cdot e}^{sq} \right) \left(\sum_{g,h} p_{g \cdot h \cdot d \cdot f}^{sq} \right) \sum_{d,f} \frac{p_{d \cdot f \cdot a \cdot b}^{sq} p_{g \cdot h \cdot d \cdot f}^{sq}}{\sum_{g,h} p_{g \cdot h \cdot d \cdot f}^{sq}}} \right) \quad (5-27)
 \end{aligned}$$

The formula (5-27) describes 16 equations where the iterators a , b , c and d each take on the states 1 and 2. The probabilities of the $a \cdot b \cdot c \cdot d$ cluster are expressed in terms of the square cluster probabilities. In addition to that, equation (5-23) is used which connects the 16 square cluster probabilities to the pair probabilities.

$$p_{a \cdot b \cdot c \cdot d}^{sq} = \frac{1}{2} \left(p_d p_{b|d} p_{c|d} \frac{p_a p_{b|a} p_{c|a}}{\sum_a p_a p_{b|a} p_{c|a}} + p_c p_{a|c} p_{d|c} \frac{p_b p_{a|b} p_{d|b}}{\sum_b p_b p_{a|b} p_{d|b}} \right) \quad (5-28)$$

Also, the correlations between the conditional pair probabilities are needed. It is recommended to express three of the conditional pair probabilities as a function of the fourth, in order to reduce the number of variables. The formulas that are given by equation (3-15) are therefore transformed into the following form.

$$\begin{aligned}
 p_{1|1} &= 1 - \frac{p_{1|2} p_2}{p_1} \\
 p_{2|2} &= 1 - p_{1|2} \\
 p_{2|1} &= \frac{p_{1|2} p_2}{p_1}
 \end{aligned} \quad (5-29)$$

The resulting system of equations consists of 36 equations and 37 variables which are the free energy A , the 4 conditional pair probabilities p_{ij} , the 16 square cluster probabilities $p_{a \cdot b \cdot c \cdot d}^{sq}$ and the 16 cluster probabilities $p_{a \cdot b \cdot c \cdot d}$. The equations (5-27), (5-28) and (5-29) can be inserted into equation (5-26) which would yield one single equation dependent on one variable ($p_{1|2}$). This equation, however, can only be minimized numerically. Due to the size of the resulting equation it is in general recommended to work with the system of equations and constrained minimization instead.

5.3.1. Comparison to Guggenheim and Monte Carlo Simulations

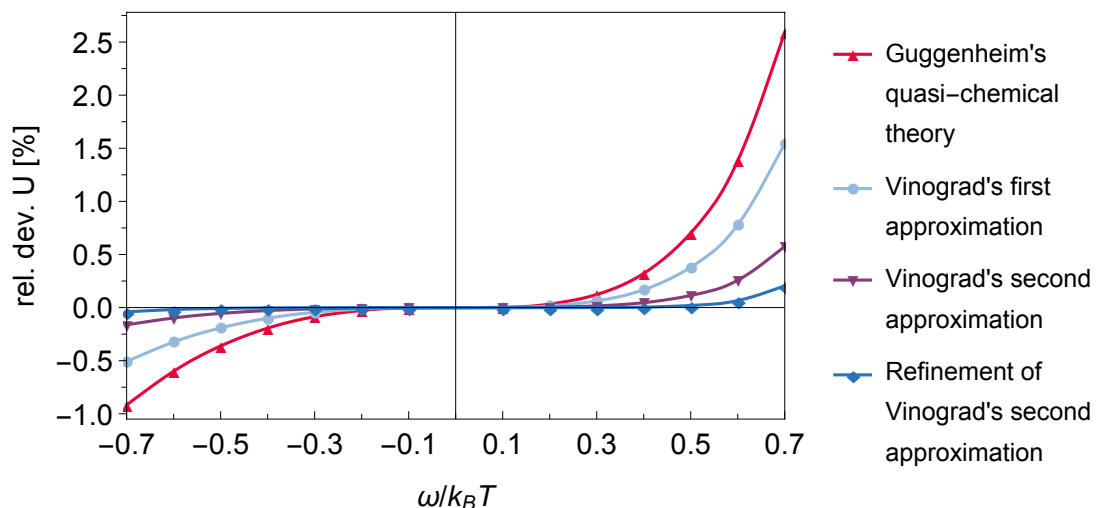


Figure 5-12.: Comparison of the 3D refinement of Vinograd's second approximation with MC-Simulations and Guggenheim: Internal Energy ($p_1 = 0.3, \varepsilon_{11} = \varepsilon_{22} = 0$, rel. dev. = $((\text{model} - \text{simulation}) / \text{simulation}) 100\%$)

Figures 5-12 and 5-13 compare all three-dimensional models with each other regarding their relative deviations to Monte Carlo simulations. Figure 5-12 depicts the relative deviation of the internal energy and figure 5-13 shows the relative deviation of the entropy.

The refinement of the second approximation has the smallest deviations of all the models and therefore is a major improvement, especially compared to the quasi-chemical theory.

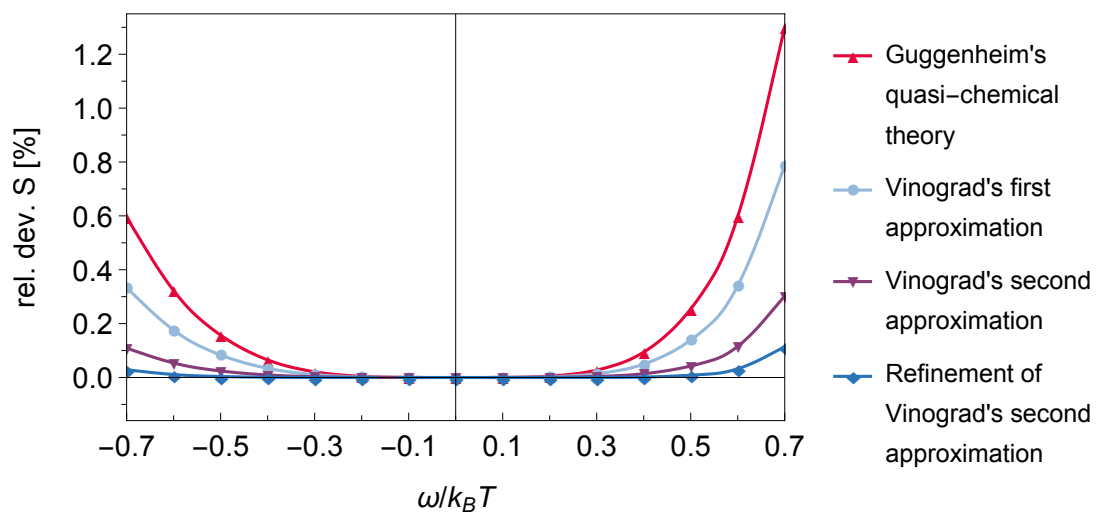


Figure 5-13.: Comparison of the 3D refinement of Vinograd's second approximation with MC-Simulations and Guggenheim: Entropy ($\rho_1 = 0.3, \varepsilon_{11} = \varepsilon_{22} = 0$, rel. dev. = $((\text{model} - \text{simulation}) / \text{simulation}) 100\%$)

5.3.2. Thermodynamic Consistency Check

The thermodynamic consistency check is performed according to the description in section 4.1.2.

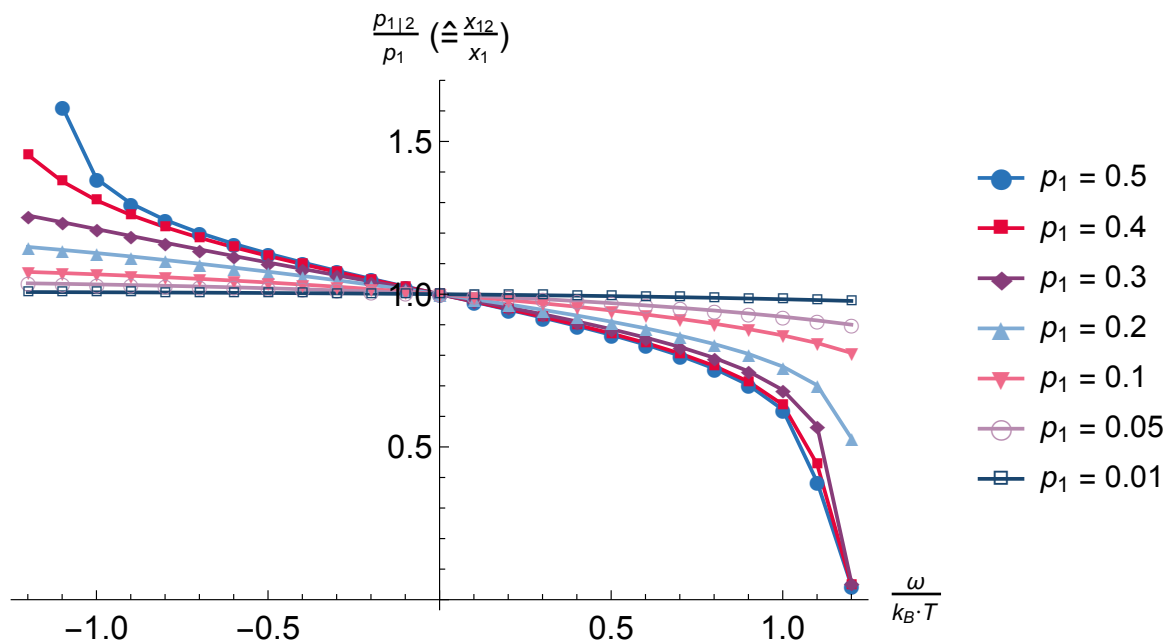


Figure 5-14.: 3D refinement of Vinograd's second approximation: $\frac{p_{1|2}}{\rho_1}$ over $\frac{\omega}{k_B T}$

Figure 5-14 illustrates this ratio of $p_{1|2}/p_1$ which can also be expressed as the ratio of the local composition to the global composition x_{12}/x_1 . The abscissa marks the dimensionless exchange energy $\omega/k_B T$ where the negative values denote an attraction between the molecules of types 1 and 2 and the positive values denote a repulsion between the two. Each line in the figure represents one global composition.

Figure 5-14 shows that the refinement of the second approximation converges even faster than the second approximation.

5.4. Comparison of Models

A brief review of the differences of the three-dimensional models is given in this section. Guggenheim's quasi-chemical theory assumes that all pairs of contacts are independent of each other. This assumption leads to higher deviations the larger the number of interactions between the sites is.

Vinograd's first approximation applied to 3D constructs the lattice by inserting molecules sequentially. Every insertion creates three contact pairs which are connected through the newly inserted site. The three neighbors are modeled to be independent of each other. These assumptions lead to asymmetric lattice probabilities. This model is a slight improvement over the quasi-chemical theory.

Vinograd's second approximation applied to 3D solves the issue of the asymmetry by averaging all construction directions of an eight site cubic cluster. Through the consideration of the cubic cluster, the neighbors of site *A* are not assumed to be independent of each other. This yields the result that Vinograd's second approximation applied to 3D shows a significant improvement over the first approximation.

The refinement of Vinograd's second approximation further improves upon the second approximation by modeling the entropy with just the nearest neighbor interactions and not partially including other interactions. Therefore this model shows the smallest deviations from the Monte Carlo simulation data.

6. Conclusion and Outlook

The comparatively small deviations of the refined Vinograd approach from Monte Carlo data suggest that this method is a promising basis for a future g^E -model that introduces more geometric information than current g^E -models. The models developed in this work describe spherical molecules of the same size in a lattice. This is the first step on the road of developing an excess Gibbs enthalpy model. The following paragraphs propose a couple of possibilities for future development projects.

The consideration of orientations regarding the molecules is a possible expansion of this model. The first step in this research is to consider dice-like molecules, each possessing multiple interaction sites, instead of spheres. These molecules already open up a wide variety of orientation dependent interactions. One example would be polar molecules.

A further expansion possibility is the consideration of polymers. Polymers can be modeled as molecules which take up multiple lattice sites.

Another possible expansion is to go beyond the lattice. There the molecules are not restricted by discrete locations. Also, different molecule sizes and shapes can be considered.

A different route of expanding this model would be to increase the number of dependencies between the molecules by taking energetic interactions of next-nearest neighbors into account.

A. List of Symbols

Symbol	Description
A	Helmholtz free energy
S	entropy
U	internal energy
g^E	excess Gibbs enthalpy
N	total number of molecules
N_i	number of molecules of component i
T	absolute temperature
V	volume
k_B	Boltzmann constant
Pr	probability function
p	probability
x_i	global composition of component i
x_{ij}	local composition of component i next to component j
z	coordination number
β	auxiliary variable
η	auxiliary variable
ε	energy of a molecule pair
ω	exchange energy
λ	Lagrange multiplier
\mathcal{L}	Lagrange function

Superscript

sq square lattice

Subscript

a, b, \dots, h molecule type at specific lattice site

i, j general iterator

List of Figures

2-1. $a \cdot b \cdot c$ cluster	3
2-2. Quasi-chemical equilibrium reaction	6
3-1. 1D chain construction - addition of site A to the end of the chain	10
4-1. 2D square lattice construction - addition of site A to the lattice	15
4-2. 2D Vinograd's first approximation lattice construction	18
4-3. Comparison of Vinograd's first approximation with MC-Simulations and Guggenheim: Internal Energy	21
4-4. Comparison of Vinograd's first approximation with MC-Simulations and Guggenheim: Entropy	21
4-5. 2D Vinograd's first approximation: $\frac{\rho_{1 2}}{\rho_1}$ over $\frac{\omega}{k_B T}$	23
4-6. Two construction directions for the 2D lattice	24
4-7. 2D Vinograd's second approximation lattice construction	26
4-8. Comparison of Vinograd's second approximation with MC-Simulations and Guggenheim: Internal Energy	29
4-9. Comparison of Vinograd's second approximation with MC-Simulations and Guggenheim: Entropy	30
4-10. 2D Vinograd's second approximation: $\frac{\rho_{1 2}}{\rho_1}$ over $\frac{\omega}{k_B T}$	30
4-11. Calculation of the a neighborhood from the square cluster	32
4-12. Comparison of the refinement of Vinograd's second approximation with MC-Simulations and Guggenheim: Internal Energy	33
4-13. Comparison of the refinement of Vinograd's second approximation with MC-Simulations and Guggenheim: Entropy	34
4-14. 2D refinement of Vinograd's second approximation: $\frac{\rho_{1 2}}{\rho_1}$ over $\frac{\omega}{k_B T}$	35
5-1. 3D cubic lattice construction - addition of site A to the lattice	37
5-2. Comparison of 3D Vinograd's first approximation with MC-Simulations and Guggenheim: Internal Energy	40
5-3. Comparison of 3D Vinograd's first approximation with MC-Simulations and Guggenheim: Entropy	41
5-4. 3D Vinograd's first approximation: $\frac{\rho_{1 2}}{\rho_1}$ over $\frac{\omega}{k_B T}$	42
5-5. Square cluster construction directions	43
5-6. Cubic cluster construction from square cluster	44
5-7. Cubic cluster construction directions	45
5-8. Comparison of 3D Vinograd's second approximation with MC-Simulations and Guggenheim: Internal Energy	48

5-9. Comparison of 3D Vinograd's second approximation with MC-Simulations and Guggenheim: Entropy	49
5-10. 3D Vinograd's second approximation: $\frac{\rho_{1 2}}{\rho_1}$ over $\frac{\omega}{k_B T}$	50
5-11. Calculation of the a neighborhood from the cubic cluster	51
5-12. Comparison of the 3D refinement of Vinograd's second approximation with MC-Simulations and Guggenheim: Internal Energy	53
5-13. Comparison of the 3D refinement of Vinograd's second approximation with MC-Simulations and Guggenheim: Entropy	54
5-14. 3D refinement of Vinograd's second approximation: $\frac{\rho_{1 2}}{\rho_1}$ over $\frac{\omega}{k_B T}$	54

List of Tables

4-1. 2D first approximation: cluster probabilities	19
4-2. 2D first approximation: asymmetry	25

References

- [1] Ferschl, F., 1970: *Markovketten*, Band 35, Springer-Verlag.
- [2] Gratias, D., Sanchez, J., Fontaine, D.D., 1982: *Application of group theory to the calculation of the configurational entropy in the cluster variation method*, *Physica A: Statistical Mechanics and its Applications*, 113(1), 315 – 337, URL: <http://www.sciencedirect.com/science/article/pii/0378437182900231>.
- [3] Guggenheim, E.A., 1944: *Statistical Thermodynamics of Mixtures with Non-Zero Energies of Mixing*, *Proceedings of the Royal Society of London A: Mathematical, Physical and Engineering Sciences*, 183(993), 213–227, URL: <http://rspa.royalsocietypublishing.org/content/183/993/213>.
- [4] Guggenheim, E.A., 1952: *Mixtures: the theory of the equilibrium properties of some simple classes of mixtures solutions and alloys*, Clarendon Press.
- [5] Kemeny, J.G., Snell, J.L., 1976: *Finite Markov Chains, Undergraduate Texts in Mathematics*, Springer-Verlag.
- [6] Kikuchi, R., 1951: *A Theory of Cooperative Phenomena*, *Phys. Rev.*, 81, 988–1003, URL: <https://link.aps.org/doi/10.1103/PhysRev.81.988>.
- [7] Kikuchi, R., 1976: *Natural iteration method and boundary free energy*, *The Journal of Chemical Physics*, 65(11), 4545–4553, URL: <http://dx.doi.org/10.1063/1.432909>.
- [8] Kikuchi, R., Brush, S.G., 1967: *Improvement of the Cluster-Variation Method*, *The Journal of Chemical Physics*, 47(1), 195–203, URL: <http://dx.doi.org/10.1063/1.1711845>.
- [9] König, L.M., 2013: *Auswertung von Monte Carlo-Simulationen zur Validierung thermodynamischer Modelle*, Bachelor's thesis, Graz University of Technology.
- [10] Mayer, C., 2015: *Kombinatorische Diskretisierung von Gittersystemen*, Bachelor's thesis, Graz University of Technology.
- [11] Pelizzola, A., 2005: *Cluster variation method in statistical physics and probabilistic graphical models*, *Journal of Physics A: Mathematical and General*, 38(33), R309, URL: <http://stacks.iop.org/0305-4470/38/i=33/a=R01>.

- [12] Pelizzola, A., 2014: *Generalized belief propagation for the magnetization of the simple cubic Ising model*, Nuclear Physics B, 880, 76 – 86, URL: <http://www.sciencedirect.com/science/article/pii/S0550321314000194>.
- [13] Pfennig, A., 2013: *Thermodynamik der Gemische*, Springer-Verlag.
- [14] Pielen, G., 2005: *Detaillierte molekulare Simulationen und Parameterstudie für ein ternäres Gemisch zur Weiterentwicklung des GEQUAC-Modells; 1. Aufl.*, , RWTH Aachen, Aachen, URL: <http://publications.rwth-aachen.de/record/60560>, zugl.: Aachen, Techn. Hochsch., Diss., 2005.
- [15] Sanchez, J., Ducastelle, F., Gratias, D., 1984: *Generalized cluster description of multicomponent systems*, Physica A: Statistical Mechanics and its Applications, 128(1), 334 – 350, URL: <http://www.sciencedirect.com/science/article/pii/0378437184900967>.
- [16] Vinograd, V.L., Perchuk, L.L., 1996: *Informational Models for the Configurational Entropy of Regular Solid Solutions: Flat Lattices*, The Journal of Physical Chemistry, 100(39), 15972–15985, URL: <http://dx.doi.org/10.1021/jp960416s>.
- [17] Wallek, T., Pflieger, M., Pfennig, A., 2016: *Discrete modeling of lattice systems: the concept of Shannon entropy applied to strongly interacting systems*, Industrial & Engineering Chemistry Research, 55(8), 2483–2492.
- [18] Wolfram Research, I., 2015: *Mathematica, Version 10.3*, Champaign, IL.
- [19] Wolfram Research, I., 2016: *Mathematica, Version 11.0*, Champaign, IL.